

Effects of Condensation on Fourier and non-Fourier Heat Transfer in Fins

Thesis submitted by

Pramod Atmaram Wankhade

Doctor of Philosophy (Engineering)

**Department of Mechanical Engineering
Faculty Council of Engineering and Technology
Jadavpur University
Kolkata, India**

2023

JADAVPUR UNIVERSITY
KOLKATA-700032

INDEX NO. - 227/16/E

- 1. Title of the thesis:** Effects of Condensation on Fourier and Non- Fourier Heat Transfer in Fins
- 2. Name, Designation and Institution of the Supervisor:** Dr. Balaram Kundu, Professor
Department of Mechanical Engineering
Jadavpur University, Kolkata-700032.

3. List of Publications:

Journals

- [i] **Wankhade, P. A., Kundu, B., & Das, R. (2018).** Establishment of non-Fourier heat conduction model for an accurate transient thermal response in wet fins. International Journal of Heat and Mass Transfer (**ELSEVIER**), 126,911-923.
<https://doi.org/10.1016/j.ijheatmasstransfer.2018.05.094>
- [ii] **Kundu, B., Das, R., Wankhade, P. A., & Lee, K. S. (2018).** Heat transfer improvement of a wet fin under transient response with a unique design arrangement aspect. International Journal of Heat and Mass Transfer (**ELSEVIER**), 127, 1239-1251.
<https://doi.org/10.1016/j.ijheatmasstransfer.2018.08.110>

- 4. List of patents:** NIL

5. List of Presentation in National/ International Conference/ Workshops/ Symposiums:

- [i] **Wankhade, P. A., Kundu, B., (2019).** Transient heat transfer analysis of an annular wet fin for dehumidification of air.5th International Conference on Advances in Mechanical Engineering (**ICAME 2019**), 17th – 19th December 2019, Yildiz Technical University, Istanbul, Turkey.

- [ii] **Kundu, B., Wankhade P.A., (2016).** Thermal Analysis of Porous Fins under Simultaneous Convection and Radiation Heat Transfer, National Conference on Advances in Thermal Engineering (**NCATE 2016**), 23rd-24th September 2016, Jadavpur University, Kolkata, West Bengal, India.

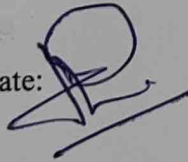
“Statement of Originality”

I, Pramod Atmaram Wankhade registered on 30th March 2016 d hereby declare that this thesis entitled “Effects of Condensation on Fourier and Non- Fourier Heat Transfer in Fins” contains literature survey and original research work done by the undersigned candidate as part of Doctoral studies.

All information in this thesis have obtained and presented in accordance with existing academic rules and ethical conduct. I declare that, as required by these rules and conduct, I have fully cited and referred all materials and results that are not original to tis work.

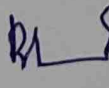
I also declare tha I have checked this as per the “Policy on Anti Plagiarism, Jadavpur University, 2019”, and the level of similarity as checked by iThenticate software is 5%.

Signature of the candidate:



Date:

Certified by Supervisor (s):


 10/13/2023.

(Signature with date, seal)

Dr. Balaram Kundu
Professor
Dept. of Mechanical Engineering
Jadavpur University
Kolkata-700032

CERTIFICATE FROM THE SUPERVISOR/S

This is to certify that the thesis entitled “Effects of Condensation on Fourier and Non-Fourier Heat Transfer in Fins” submitted by Shri Pramod Atmaram Wankhade, who got his name registered on 30th March 2016 for the award of Ph. D. (Engg.) degree of Jadavpur University is absolutely based upon his work under the supervision of **Dr. Balaram Kundu**, Professor, Mechanical Engineering Department, Jadavpur University and that neither his thesis nor any part of the thesis has been submitted for any degree/ diploma or other academic awards anywhere before.

 10/3/2023.

Dr. Balaram Kundu
Professor
Dept. of Mechanical Engineering
Jadavpur University
Kolkata-700032

Dr. Balaram Kundu, Professor

Department of Mechanical Engineering

Jadavpur University, Kolkata-700032. India

(Signature of Supervisor and date with office with seal)



*Dedicated to my
beloved Aai - Baba....!*

Acknowledgement

The completion of this Ph.D. thesis marks the culmination of three years of dedicated effort, and it would be remiss not to express my deepest gratitude to those who have been instrumental in this journey.

Foremost, I extend my sincere appreciation to my supervisor and mentor, Dr. Balam Kundu, Professor in the Department of Mechanical Engineering at Jadavpur University. His unwavering dedication to research, infectious enthusiasm, indomitable spirit, and dynamic approach have left an indelible mark on my academic and professional growth. I am profoundly thankful for his insightful guidance, motivational advice, and for broadening the horizons of my career. This thesis owes much of its depth and quality to Prof. Balam Kundu's unconditional support.

I am also indebted to my esteemed co-authors, Dr. K.S. Lee and Dr. Ranjan Das, whose collaborative efforts significantly contributed to the progress and publication of this work. Special thanks to the Heads of the Mechanical Engineering Department at Jadavpur University for providing the necessary facilities that facilitated the successful completion of my research.

My heartfelt thanks go to the wonderful friends - lab colleagues who made my tenure at the Heat Power Lab at Jadavpur University enjoyable. Dr. Kuntal Jana, Dr. Sudhir Ch. Murmu, Dr. Jaydeep Dutta, Jaynarayan Sir, Amit da, Sayan da, Saumitra da, Sujit da, Ms. Monali, Ms. Anukampa mam, and other laboratory colleagues, along with the technical staff of Heat Power Lab, who have been invaluable in their continuous support from the inception of this journey.

I express my gratitude to the Board of Governors, Directors of VJTI, and Heads of the Mechanical Engineering Department, Mumbai, for their support and granting me study leave under AICTE's - QIP scheme. Special thanks to my institute colleagues, particularly Prof. Pravin N. Deshmukh, Dr. N.P. Gulhane, Dr. S.A. Mastud, and Dr. V.B. Suryawanshi, and close friend Dr. Pramod M. Bagade for their unwavering support and cooperation.

A heartfelt acknowledgment goes to my sister Malu-tai and brother-in-law Dr. Pralhad G. Waware for their continuous moral support.

In a moment of deep gratitude, I dedicate this thesis to my beloved parents, late Shri Atmaram S. Wankhade and late Smt. Venutai A. Wankhade.

Lastly, to my constants - my wife, Darshana; daughter, Vidhi; son, Siddhant; and beloved elder brother, Sudhir-Da, and sister, Mangala- tai.

Pramod Atmaram Wankhade

(Signature)

Abstract

Investigating the effects of condensation in transient heat conduction analysis under the dehumidifying condition on a wet fin surface, especially considering the thermal relaxation time, is crucial as it may expand a new dimension in the field of heat transfer. Researchers have pointed out the limitations in the conventional Fourier heat conduction model in the last few decades. In physical nature, heat wave propagation takes a definite time duration, called the thermal relaxation time. This realistic behavior of thermal waves brought out an arena for researchers to focus on this thermal relaxation time because of its essential applications in upcoming fields like in composite fin heat transfer where the fin size is too small, and the thermal relaxation occurs for a concise duration. Some other direct-indirect application covers thermal treatment for cancer patients, laser welding, bio-heat transfer, high-speed aviation engines, refrigeration and air conditioning, nuclear reactors, etc. The extended surface, called fins, is widely used as evaporative coils in refrigeration and air conditioning applications when the moisture in the air condenses on the fin surface as the fin temperature maintains below the dew point temperature of surrounding humid air. For efficient heat transfer and to enhance the rate of heat transfer from the fin surface, fins of various geometries and designs are being used in multiple applications. Given this, the author proposed one novel fin design for better fin performances under various boundary conditions.

Looking at the emerging application, the composite mini-micro size fin designs with a minimal thermal relaxation time might be essential in the near future task. This research aims to develop an analytical tool to analyze the temperature distribution on condensed fin surface with different fin geometries under various thermos-physical parameters under dehumidification. The present study considers the influence of parameters like Vernotte number, Biot number, and different boundary conditions for transient heat conduction.

In this thesis, an analytical solution called the Separation of variables has been developed with modified boundary conditions about practical aspects than existing research work. Fourier and non-Fourier analyses are carried out on wet fin surfaces to understand the effect of thermal relaxation time in different cases. Apart from this, the present study is not limited to conventional rectangular and pin fins profiles. Still, the author has attempted a unique revolutionary fin design, and researchers have yet to try it to improve heat transfer enhancement.

The research outcome has pointed out that the fin efficiency with the dry surface is always more than the wet surface fin condition for the equal Biot number at the base. The condensation on the fin surface amplifies the magnitude of the temperature response curve, thereby taking more thermal relaxation time. The non-Fourier heat conduction analysis shows a notable deviation in temperature response compared to Fourier heat conduction. It demonstrates that the proposed new fin design arrangement enhances the heat transfer rate and provides a compact fin design solution to save space and manufacturing costs.

The results obtained from the analytical model are well-verified with existing numerical and analytical research papers. The present work also compares those with the published work and is found to be well within engineering accuracy requirements.

TITLE OF THE THESIS

Effects of Condensation on Fourier and Non- Fourier Heat
Transfer in Fins

Contents

	Page No.
Abstract	i-ii
Title of the Thesis	iii
Contents	iv-v
List of Figures	vi-vii
Nomenclature and Abbreviations	viii-x
Chapter-1: Introduction	1-6
1.1 Brief Background	1
1.2 Heat and mass transfer in fins	2
1.3 Fin surface condensation	3
1.4 Transient Heat conduction in Fins	4
1.5 Organization of the thesis	5
Chapter-2: Review of Literature Survey	7-24
2.1 Introduction	7
2.2 Necessity of non- Fourier Heat Transfer study in wet fins	8
2.3 Different fin geometries and research works	10
2.4 Non- Fourier heat conduction model- Analytical Approach and Methodology	15
2.5 Research Gap	20
2.6 Objective of the thesis	23
Chapter-3: Establishment of non- Fourier heat conduction model for the transient thermal response in wet fins.	25-51
3.1 Introduction	25
3.2 Mathematical formulations	26
3.3 Result and Discussion	36
3.4 Validation of the present research work	36
3.5 Non-Fourier heat conduction model for transient thermal response in wet fins	41

Chapter-4: Heat transfer improvement of a wet fin under transient response with a unique design arrangement aspect.	52-77
4.1 Introductions	52
4.2 Mathematical formulations	53
4.3 Results and discussion	63
4.4 Validation of the present research work	63
4.5 A novel fin design approach for heat transfer improvement	66
Discussion on reasons of getting higher amplitudes on responses for low Fourier numbers for both geometries under wet conditions	78-79
Chapter-5: Conclusion	80-81
Future Scope	82
References	83-91

List of Figures

Fig. No.	Fig. Caption	Page No.
Figure 1.1	Fins-Basic types	2
Figure 3.1	Schematic diagram of fins	26
Figure 3.2	Validation of the present study for a high value of τ with its steady condition	38
Figure 3.3	Results obtained from the present analytical analysis and numerical analysis	39
Figure 3.4	Mean temperature in a fin as a function of Fourier and Biot numbers	40
Figure 3.5	Heat transfer in a fin for dry and wet surfaces	43
Figure 3.6	Heat transfer as a function of Fourier and Vernetto numbers for dry and wet surfaces	44
Figure 3.7	Heat transfer as a function of Fourier number and tip Biot number for dry and wet surfaces	46
Figure 3.8	Heat transfer and fin efficiency as a function of tip Biot number for dry and wet surfaces	48
Figure 3.9	Heat transfer and fin efficiency as a function of base Biot number	50
Figure 4.1	Schematic diagram of longitudinal and pin fins with asymmetric cooling on both the ends	53
Figure 4.2	Comparison of temperature distribution in fins obtained from the present work and the published work for consideration of the dry surface having a single base	64
Figure 4.3	Comparison of the temperature distribution in wet fins predicted by the present analysis and numerical methods	65
Figure 4.4	Non- Fourier temperature distribution in wet fins as a function of dimensionless time, τ	67

Figure 4.5	Fourier and non-Fourier temperature response in fins as a function of different design conditions	69
Figure 4.6	Fin efficiency for non-Fourier heat transfer	71
Figure 4.7	Fin effectiveness for non-Fourier heat transfer	73
Figure 4.8	Comparison of temperature distribution in wet fins between present and conventional cases at $V_e = 0.5$ and $\tau = 1.0$	74
Figure 4.9	Comparison of average temperature of dry and wet fins as a function of Fourier number between present and conventional cases for $V_e = 0.5$	75
Figure 4.10	Comparison of heat transfer rate in wet fins as a function of Fourier number between present and conventional cases for $V_e = 0.5$	77

Nomenclature and Abbreviations

A	dimensionless humidity parameter.	$U(X)$, $V(\tau)$	function depend on X and τ for fin with convection base condition
A_1, A_2, A_3, A_4	dimensionless variables defined in equations. Eq(3.12). (4.10)	V_e	Vernotte number
A_c	fin cross section area (m^2)	W	width of longitudinal fin (m)
B	condensation parameter ($^{\circ}C^{-1}$)	x	coordinate starting from fin base (m)
Bi	Biot number, ht/k .	X	dimensionless coordinate x/L
Bi_0	Biot number at fin base, ht_b/k .	X_m	location of X having a minimum dimensional temperature (m)
Bi_t	Biot number at fin tip, ht_{tip}/k .	Z_0, Z_1	fin parameter, see Eq. (3.6)
Bi_1	Biot number at the first primary surface, h_1L_1/k		
Bi_2	Biot number at the second primary surface, h_2L_2/k		
C_j	dimensionless constant which is dependant on eigen value Eq. (4.16a)	α	thermal diffusivity (m^2s^{-1})
C_0	dimensionless notations used in equation. Eq. (3.4)	α_n	variable defined in Eq. (3.15b)
C_p	specific heat ($J kg^{-1} K^{-1}$)	β_j, β_n	dimensionless variable defined in Eq. (3.16)
D_0, D_1, D_2, D_3, D_4	notations used in Eqs. (3.18), (4.15a)	$\Gamma(X)$	spatial function Eq. (4.9a)
E_0, E_i, E_j	variables used in Eqs.(3.18a), (4.15b)	Γ_1, Γ_2	dimensionless notations defined in Eqs. (3.18f), (3.18g)
$E(X), F(\tau)$	functions depend on X and τ for isothermal base condition	λ_n	Eigen values, see Eq. (3.15a)
F	Fourier number	η	fin efficiency
G_j	variables defined in Eq. (4.15c)	ϕ	dimensionless fin temperature
E, E_0	parameter used in Eqs. (3.12) and (3.17d) respectively	ϕ_b, ϕ_0	dimensionless fin base temperature
h	convection heat transfer coefficient ($W m^{-2}K^{-1}$)	ϕ_m	dimensionless average fin surface temperature
h_L	convective heat transfer at the base surface ($W m^{-2}K^{-1}$)	ϕ_t	dimensionless fin tip temperature
h_1, h_2	Convective heat transfer coefficient at first and second primary surfaces respectively ($W m^{-2}K^{-1}$)	ϕ_L	dimensionless fin base temperature
h_{fg}	latent heat of condensation of moisture (Jkg^{-1})	θ	dimensionless local fin surface temperature
h_m	mass transfer coefficient ($kg m^{-2} s^{-1}$)	θ_b	dimensionless fin base surface temperature

Greek letters

h_t	convective heat transfer at the tip surface ($W m^{-2}K^{-1}$)	θ_d	dimensionless dew point temperature
I, j	integer numbers	θ_m	dimensionless mean fin surface temperature
I_n, J_n	dimensionless variable defined in Eqs. (3.18a), (3.18e)	θ_L	dimensionless temperature of base II
k	thermal conductivity ($W m^{-1} K^{-1}$)	θ_p	dimensionless temperature parameter
L	fin length as shown in Fig.1.1 (m)	θ_t	dimensionless fin tip temperature
m, n	parameter used in Eq. (3.2) and (3.4)	Ω	function used for separation of variables
L_e	Lewis number	ψ	fin aspect ration
p	Fin perimeter (m)	ζ	dehumidification parameter
q	actual heat transfer rate (W)	ω	specific humidity of saturated air adjacent to the fin surface
Q	actual dimensionless heat transfer rate, (W)	ω_a, ω_∞	specific humidity of surrounding air
t, t'	time (s)	ω_d	specific humidity of surrounding air at dew point temperature
t^*	dimensionless geometry t_f/W	ρ	density of fin material (kgm^{-3})
T	local fin surface temperature ($^{\circ}C$)	τ	Fourier number
T_a, T_∞	ambient temperature ($^{\circ}C$)	τ_r	thermal relaxation time (s)
T_b	fin base temperature ($^{\circ}C$)		
T_d	dew point temperature ($^{\circ}C$)		
T_L	fluid temperature at base for convected condition ($^{\circ}C$)		
T_m	mean fin surface temperature as a function of Fourier number ($^{\circ}C$)		
T_r	reference temperature at base and fin tip ($^{\circ}C$)		
T_t	fin tip temperature ($^{\circ}C$)		
T_1	base temperature at primary surface I for isothermal base temperature or cold fluid temperature adjacent to the base surface I for convection boundary condition ($^{\circ}C$)		
T_2	base temperature at primary surface II for isothermal base temperature or cold fluid temperature adjacent to the base surface II for convection boundary condition ($^{\circ}C$)		
α	variable defined in Eq (17g)		
β	variable defined in Eq (15)		
η	fin efficiency (dimensionless)		

ϕ	dimensionless local temperature, $\theta + \theta_p$
ϕ_0	notation used in Eq. (4.5e)
θ	dimensionless temperature difference, $(T_a - T)/(T_a - T_b)$
θ_p	dimensionless temperature parameter, see Eq. (3.6)
ω	specific humidity of saturated air adjacent to the fin surface (kg of water vapor per kg of dry air)
ξ	dehumidification parameter, $h_{fg}/C_p Le^{2/3}$ ($^{\circ}C$)
Ω	variable defined in Eqs. (3.9b), (4.7b)

Subscripts

a	air
b	fin base

CHAPTER-1

Introduction

1.1 Brief Background

The temperature difference between bodies is the essential requirement and main driving force for transferring heat between two bodies. There can be no net heat transfer between two bodies that maintain at the same temperature. The heat transfer rate in a specific direction depends on the magnitude of the temperature gradient in that direction. The larger the temperature gradient, the higher the rate of heat transfer. We start our day using equipment, gazettes, and devices, including energy interactions, especially heat transfer. In today's era, imagining a world without heat transfer applications is almost impossible.

Heat transfer frequently notices in many applications and other aspects of life, engineering applications like car radiators, solar heat collectors, and heat exchangers. Various equipment in power plants, spacecraft, and internal combustion engines are some examples in which heat transfer involves essentially.

In modern-day technology, heat transfer applications are not limited to a conventional area of engineering but also used for carrying out thermal treatment, laser surgeries, laser beam welding technology, spacecraft, and cooling of modern micro and tiny-size electronic chips for faster processing. The emerging area in fin heat transfer, is the use of composites materials for fin manufacturing, the micro size fin geometries in such applications has vital role in fin heat transfer. The thermal analysis of these fins becomes important as the fin size and thermal

relaxation time in such case is very small. These recent technological advancements in heat transfer area are not only limited to energy transfer but also have a notable contribution to compact equipment design, reducing the overall size, cost, and space in many applications.

1.2 Heat and mass transfer in fins

Worldwide, researchers are attempting heat transfer problems to limit the overheating of various equipment so as to increase its life and work efficiency. Extended Surfaces, commonly called fins are being extensively used to enhance the heat transfer rate from the fin surface to surrounding fluid by minimizing the temperature difference between the heat sources and surrounding fluids. Engineers have been continuously designing fins profiles in the most compact form with optimized shape for efficient heat transfer. New fin designs and optimum fin shapes are at the epicenter in many of the research work [1]. Depending upon the specific application and surrounding environmental conditions the fins are suitably selected from their basic geometric forms as shown in Figure 1.1.

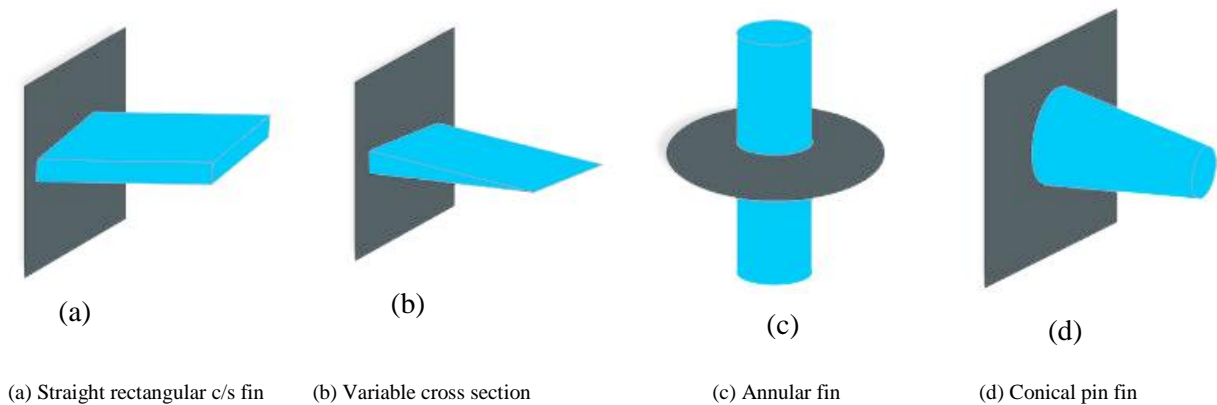


Fig. 1.1 Fins-Basic types

Researchers are working for the optimum fin design and efficient heat transfer by altering the thermo-geometrical properties of fins in various atmospheric conditions [2-6]. The upcoming refrigeration and air conditioning applications require new changes in fin design, which can transfer heat efficiently under low-temperature ranges. With rapid industrialization, this problem is not limited to heat transfer but also involves the mass transfer phenomena as the moisture in the surrounding air condenses on the fin surface [7]. Finned heat exchangers are commonly used in air conditioning, refrigeration, and process heat transfer where the temperature of the fin is lower and dehumidification on the fin surface results in the accumulation of moisture on it. Thus, the mass transfer takes place simultaneously with the heat transfer.

1.3 Fin surface condensation

In refrigeration and air conditioning applications, the fin base temperature is kept at a lower value than the dew point temperature of the surrounding air, which strikes the fin surface forming a thin saturated moisture layer on it, responsible for the heat mass transfer process.

The moisture condenses on the fin surface in film-wise, dropwise, or mixed mode depending on the condition of the surface. Generally, a clean surface promotes film-wise condensation, whereas a treated surface condenses dropwise. For all the cases, the condensing surface is covered with a thin layer of moisture as the condensation takes place continuously over the fin surface, and condensed liquid is removed from it due to the motion generated by gravity.

The difference in temperature between the surrounding air and the fin surface is the driving force for sensible heat transfer, and the difference in humidity ratio between the surrounding air and adjacent air on the fin surface is the force for the mass transfer.

1.4 Transient Heat conduction in Fins

Transient heat transfer analysis has, over a couple of decades' history as it dealt with the thermal relaxation time, which was ignored by conventional Fourier's law of heat conduction. Transient heat conduction is gaining considerable attention because of its increasing applications in cryogenic engineering and treatments. These applications require a specific heat source intensity for a particular time; hence the thermal relaxation time in heat wave propagation is gaining wide attention. The basic purpose of transient heat conduction analysis is to use this thermal response time in such applications. The conventional heat flux model proposed by Fourier has limitations and does not consider this thermal relaxation time. Various researchers observed this realistic heat wave propagation behavior and suggested alterations in conventional Fourier's heat conduction law [8-9].

Using Laplace transforms, Suryanarayana [10] has obtained a solution for transient heat transfer analysis on dry straight fins with isothermal and constant heat flux boundary conditions. Cho and Juhng [11] considered the thermal wave characteristics of the heat flux in a finite slab subjected to periodic surface heating for non-Fourier heat conduction analysis. The study on various parameters of the thermal shock location shows that relaxation time greatly influences the temperature distribution on the fin. Monte [12] analyzes transient heat

conduction in one-dimensional composite slabs to sudden variations in the surrounding temperature. Kundu and Lee [13-14] used an analytic technique to evaluate the thermal response in fins with different geometries and internal heat generation described by Fourier and non-Fourier laws. The temperature response of the non-Fourier model from the Fourier system was studied with several possible design variables viz, Fourier and Vernotte numbers.

In any heat transfer application, a transient response always exists during the initial time phase, resulting in unsteady heat transfer. In air conditioning and refrigeration applications, the moisture in the surrounding air deposits on the fin surface in condensate, thus adding resistance to the heat wave propagation and resulting in transient heat conduction behavior. Many researchers have carried out many studies on the transient heat transfer analysis on various problems of fins.

1.5 Organization of the thesis

The present thesis comprises of the following chapters.

- **Chapter 1.** It covers a brief introduction and background of the subject, the effective and efficient way to transfer heat by extended surfaces called fins. Various applications where fins are being used in different environmental conditions. The dehumidification of air thereby forms a thin layer of condensate on the fin surface, and its effect on heat transfer is collectively called heat and mass transfer influences. Summarisation of fin research works was done on transient heat conduction models. A short introduction

about the need for transient heat conduction models highlights in view of futuristic applications.

- **Chapter 2.** This section illustrates a detailed literature survey in the past couple of decades till the recent work carried out in transient heat transfer with different thermophysical conditions and fin geometry, the enhancement of heat transfer techniques developed by various researchers till recent years.
- **Chapter 3.** This chapter deals with the actual work in the transient heat conduction model considering rectangular and pin fin geometries aiming at the scope of improved fin performances under dehumidification. The finding of the study is summarised under result and discussion section.
- **Chapter 4.** This chapter attempted a novel fin design considering rectangular and pin fin geometry. The results of this study proved that the novel fin design approach is best suited for the application where limited space with better fin performance is of prime focus. The transient heat conduction model covers both geometries with the effect of condensation in a humid atmosphere. The observations made during the study are presented in results and discussion section.
- **Chapter 5.** This section covers the conclusion part. The important and common observations obtained from the research are presented here in conclusive points.
- **Chapter 6.** This section covers the future scope of the work.

CHAPTER-2

Review of Literature Survey

2.1 Introduction

The conventional heat conduction theory proposed by Fourier has some limitations and does not consider the thermal wave relaxation time. In special cases of physical nature, the thermal waves do not travel with infinite speed, and hence such problems need to tackle by using different approaches. Fourier's heat conduction model is limited, but the non-Fourier model tackles this by considering the speed of propagation of heat waves with a finite value. This realistic nature of the heat wave propagation was observed by various researchers from time to time, and they proposed some of the crucial alterations in conventional Fourier's heat conduction law [6,7]. This realistic behaviour, called the transient heat conduction model, has gained considerable attention and greatly impacted recent research work in heat transfer. Its increasing applications in upcoming areas have a broad spectrum, and cryogenic engineering and medical treatments are a few of them.

Many applications require a specific heat source intensity and specific time duration. This time duration is called thermal relaxation time in heat wave propagation and has a broader scope from the research point. The transient heat conduction study's primary aim is to use this thermal response time in various boundary conditions and applications. In refrigeration and air conditioning applications, many researchers have widely used the classical approach using

Fourier's law of heat conduction. However, only a few researchers attempted the non-Fourier approach for analyzing heat transfer through fin surfaces under dehumidifying conditions, called the transient heat conduction model.

The detailed literature survey below will cover all the aspects of the transient heat conduction model, comparing them with the Fourier heat conduction mode. The extensive literature survey also covers the new fin designs geometries for efficient heat transfer rate, fin performances, and fin efficiencies used in various applications subjected to different boundary conditions.

2.2 Necessity of non- Fourier Heat Transfer study in wet fins

Finned surfaces are exposed to different weather conditions, such as, in the cooling of electronic equipment, nuclear reactors, high-speed engines, and refrigeration applications. Simultaneous heat and mass transfer occur as the thin layer of condensate accumulates over the fin surface due to dehumidification of the surrounding air.

The moisture condenses on the fin surface in film-wise, drop-wise or mixed mode, depending on the condition of the fin surface. Generally, a clean surface promotes film-wise condensation, whereas a treated surface condenses drop-wise. For all the cases, the condensing fin surface is covered with a thin layer of moisture in condensate, which takes place continuously. However, owing to the build-up of a very thin condensate film with the boundary layer in the dehumidification process, the resistance to heat transfer through the condensate film is negligibly small. Thus, it has been omitted by many researchers. Condensation of

humid air on the fin surface occurs when the fin surface temperature is maintained below the dew point temperature of the surrounding air. This condensed water on the fin surface makes heat transfer analysis complicated.

The literature survey has reported extensive research to explore better fin performance under dehumidifying conditions. Kundu and Lee [13] used an analytical technique to evaluate the thermal response described by Fourier and non-Fourier laws of heat conduction on dry fins of different geometries with internal heat generation. The comparison between temperature responses of the non-Fourier model against the Fourier model is highlighted to design parameters such as Fourier and Vernotte numbers. Ahmadikia and Rismanian carried out a study on analytical solution of non-Fourier heat conduction problem on a fin under periodic boundary conditions. Huang and Tsai [15] carried out a three-dimensional transient inverse heat transfer analysis to determine the heat transfer coefficient in a plate fin. Kundu and Barman [16] conducted an analytical study on the design analysis of an annular fin with fully wet fin conditions subjected to simultaneous heat and mass transfer mechanisms.

Threlkeld [17] calculated the efficiency of wet fin enthalpy difference as the driving force for the combined heat and mass transfer by assuming the Lewis number equal to one [5] [18 – 19]. A linear relation between enthalpy and the temperature of the saturated air was assumed in his study. McQuiston [20] used the difference in the humidity ratio between the incoming air and that existing on the fin surface as the driving force for mass transfer. Wu and Bong [21] gave closed-form expression for the efficiency of a straight fin under both full-wet and partially-wet conditions by using the temperature and humidity ratio differences as the driving forces for

heat and mass transfer, assuming a linear relationship between the humidity ratio of the saturated air on the wet surface and the local fin temperature. Kundu [22–24] studied the effect of dehumidification of air on the performance and optimization of straight tapered fins and used the Lagrange multiplier technique to optimize the dimensions and studied the effect of dehumidification of air on the performance for straight taper fins. The analysis shows that the temperature distribution, the fin efficiency and the fin effectiveness are strongly dependent on the conditions (dry and wet) of surfaces of the fin and relative humidity of air does not have significant effect on this parameter. Hatami and Ganji [19] investigated temperature distribution equations and refrigeration efficiency for fully wet circular porous fins with variable cross sections using a new wet parameter, which can be calculated without knowing fin tip conditions. It assumes that the heat and mass convective coefficients vary with fin temperature and heat transfer through porous media. The paper's main conclusion is that a high fin efficiency can be achieved using rectangular fins instead of convex and triangular sections. All the above research work extensively covers the necessity of further research work on wet fins to enhance the fin performance and efficiency under the effect of dehumidification.

2.3 Different fin geometries and research works

This section covers a detailed survey of various research works concerning fin geometries, fin operating conditions, its uses, and different boundary conditions under the effect of condensation. Sobhan et al. [25] made an experimental analysis on an array of horizontal fins undergoing unsteady free convection heat transfer. Su and Hwang [26] considered the pin fin

in a cylindrical coordinate system for a transient heat transfer study and used the separation of variables method. An analysis was carried out by Sharqawy and Zubair [27] to study the efficiency of a straight rectangular fin with a uniform cross-section area and used actual psychrometric correlations of air and water vapor mixture.

Much research has been conducted on fin efficiency and performance with simultaneous heat and mass transfer [13],[20–22]. Other works for investigation on fin efficiency and improvement in heat transfer rate are reported in literature[4], [28–32]. Kundu [20] suggested the new geometries for the fin by highlighting that the tip of a uniform cross-sectional (UC) fin does not actively transfer heat as its rate decreases with an increase in fin length. The study pointed out that the longitudinal and pin fin of the SRC profile utilizes fin material effectively. The study focused on determining fin performance for both longitudinal and pin fins of the SRC profile under dry, partially wet, and fully wet conditions. After investigating the effect of various design and psychrometric parameters on the SRC fin performance, it was compared with the corresponding UC fin. The results show that the optimum values of the Biot number and aspect ratio of SRC fins increase with an increase in relative humidity for the same fin volume and an increase in the slow heat transfer rate with the relative humidity.

The porous wet fins were also studied to calculate the fin efficiencies with different combinations of fin geometries [14] ,[21]. Most researchers [1],[22-23] considered the existing fin geometries with different boundaries conditions and shape optimizations for fin performance analysis. Sharqawy and Zubair [33] proposed an analytical solution for efficiency

and optimization of an annular fin under wet conditions. Huang and Chung [23] used the conjugate gradient method to determine the optimum shape of fully wet annular fins for maximum fin efficiency.

Chein and Jiin [34] made a two-dimensional comparative study on the circular and elliptical-shaped fin with a dry and wet surface. They concluded that the major-to-minor axis ratio of elliptical fins has about 4-8% influence on fin efficiencies compared to dry surface fins of the same shape. Mosayebidorcheh et al.[35] used different profiles of longitudinal fins with variable cross-section area and internal heat generation for transient thermal analysis with the help of differential transform and the finite difference method.

Lin and Jang [5] made the two dimensional heat conduction analysis of dry, partially wet and fully wet conditions of an elliptic fin and concluded that the elliptic fins are 4-8% more efficient than circular fins. Vishwakarma et al.[36] used a new gridless discretization technique called smoothed particle hydrodynamics (SPH) to simulate and analyze the non-Fourier heat conduction. Using different boundary conditions for heat conduction in a slab and studying the results, the non-Fourier heat conduction has been used to simulate a one-dimensional problem. It was observed that the temperature profile at the convective end does not change with the convection coefficient. There is a periodic nature for amplitude at the output with a variation in the source frequency for non-Fourier heat conduction. Mostafa et al. [37] Carried out the numerical analysis on different profiles of annular fins for determination of efficiency and temperature distribution using actual psychrometric relations and obtained numerical solution for temperature distribution using a finite difference successive over-relaxation method for

fully wet and partially wet fin surfaces. Later on Cho and Juhng [38] considered the thermal wave characteristics of the heat flux in a finite slab subjected to periodic surface heating for non-Fourier heat conduction analysis.

Mustafa and Zubir [27] analyzed the fin efficiency of a straight rectangular fin of the uniform cross-section under dehumidifying conditions on dry, fully wet, and partially wet surfaces. Instead of conventionally used linear approximate correlations, the actual psychrometric correlations of the air-water vapor mixture were used to simulate the relationship between the temperature and humidity ratio. The study also focused on the optimum thickness of the fin for specific operating conditions. It finds that the linear model for the relationship between the humidity ratio and the temperature used by Wu and Bong has a reasonable engineering approximation for small values of the fin parameter and at low relative humidity.

Kundu and Lee [39] developed an analytical method to determine the minimum fin shape of wet fins subjected to variable heat transfer coefficients. The effect of various design parameters like fin base temperature, relative humidity, surrounding temperature, and surrounding pressure are studied to identify the dependent variable affecting minimum envelop shape to transfer energy efficiently. The analysis also shows the influence of variable heat transfer coefficient on temperature distribution and profile shape to optimize the envelop shape criterion. Lastly, a simple method is highlighted to produce a new profile by choosing a constant tip temperature to improve the shape near the tip to ease the manufacturing process.

Abdurrahman et al.[40] investigated a numerical scheme for the optimal dimensions of annular

fins of constant and variable cross-section area when subjected to heat and mass transfer. A non-linear model representing heat and mass transfer mechanisms was solved using a finite difference over-relaxation scheme. Numerical solutions are obtained for dimensionless heat transfer rate for completely wet conditions as a function of important dimensionless parameters for annular fins.

Turkyilmazoglu [18] analyzed the combined heat and mass transfer mechanism due to the differences in temperature and humidity ratio and their influence on the efficiency of different exponential-type porous fin configurations. A comparative study shows the tip temperature and efficiency of the exponential porous fins are much better than corresponding straight porous wet fins, as porosity leads to a better fin efficiency. Worachest et al.[41] proposed the finite circular fin method (FCFM) for analyzing the performance of fin-and-tube heat exchangers having basic fin configurations under dehumidifying conditions. After considering dry, partially wet, and fully wet surface conditions, it observes that sensible heat transfer performances and mass transfer performance are insensitive to changes in fin pitch with different configurations.

Elshafei [42] conducted experiments on circular pin fin heat sinks subjected to natural convection with the influence of its geometry. For all tested hollow/perforated pin fin heat sinks, the sideward-facing orientation performance was better than that for upward orientation.

Hazarika S.et al. [43] adopted the Adomian decomposition method to solve the non-linear equation in a T-shaped fin. The thermal performance and optimization analysis has been carried out on a wide range of thermo-psychometric and geometric parameters for a constructal

T-shaped fin. Sertkaya et al.[44] investigated experimentally that the orientation of the fin plate either downwards or upwards from the vertical axis with different angles has an effect on fin performance and found that up-facing pins fins enhance more heat transfer than the down-facing pin fins.

2.4 Non- Fourier heat conduction model- Analytical Approach and Methodology

The main objective of this work is to provide a non-Fourier analytical solution for the temperature distribution and fin efficiency of the rectangular, pin, and annular fins under dehumidifying conditions by using the temperature and humidity ratio differences as driving forces for heat and mass transfer. A method called separation of variables is used for this analysis.

Recently, Kundu et al. [45]] established a modified one-dimensional and two –dimensional models for two directional heat conduction in a wet fin assembly to determine the performance and temperature distribution of wet fin. Singh et al. [46] reported the Laplace transform method-based analytical solution of Fourier and non-Fourier heat transfer in dry longitudinal fins subjected to periodic boundary conditions and volumetric internal heat generation. Kundu and Miyara [47] established an analytical solution using the Adomian decomposition method to determine the performance of a fin assembly under the dehumidification of air.

Iman Rahbari et al. [48-49] investigated non-Fourier heat conduction phenomena in a finite slab with insulated boundaries. A new high-order numerical approach, Laplace transform inversion, is used to solve the hyperbolic heat conduction equation. The results show that

increasing Vernotte number causes the hyperbolic property of the equation to emerge, which magnifies reciprocating wave-like motions of heat transfer. Additionally, the medium's step and triangular heat pulses were studied to reveal temporal and spatial non-Fourier heat conduction characteristics. Sabbaghi et al. [50] made a mathematical analysis of the efficiency of semispherical fins subjected to simultaneous heat and mass transfer mechanisms. A linear relationship has been proposed for the humidity and temperature of the semispherical fin. The paper also stated that the driving forces for heat and mass transfer are the temperature and humidity ratio.

Mosayebidorcheh et al.[35] attempted the transient thermal analysis of longitudinal fins of different profiles with variable cross-section area and internal heat generation using the differential transform method (DTM) and finite difference method (FDM). The power-law temperature-dependent model was used for the simulation of different types of heat transfer, such as laminar film boiling, natural convection, nucleate boiling, and radiation. The thermal conductivity and internal heat generation were assumed as a linear function of temperature. The effects of physical parameters such as fin profile shape, thermal conductivity, convective heat transfer coefficient, and internal heat generation were studied, and it was found that the fin surface temperature is dependent on the type of heat transfer.

Kundu and Lee [39] investigated an appropriate analytical method based on the differential transform method to determine the temperature efficiency and optimize wet fins of different profiles with temperature-dependent thermal conductivity and heat transfer coefficient. The

mass transfer phenomena were considered by adopting the humidity ratio as a polynomial function with fin surface temperature. The effect of a wet surface, variable conductivity, and the heat transfer coefficient of different profiles were studied. It finally concluded that the heat transfer rate at the optimum condition depends significantly on the heat transfer coefficient for dry and wet surface conditions.

Kundu and Barman [16] analytically demonstrated the performance and optimum design of wet annular fin assemblies of trapezoidal profiles. The performance parameters, namely, the surface efficiency and augmentation factor, were determined using the Frobenius power series method to solve the governing differential equation. Two approaches have been adopted depending on the psychrometric properties at the tip. Finally, it was observed that the performance and optimum conditions of wet fin assembly rely not only on the psychrometric properties of air but also on the approach selected for calculating the energy transferred by the mass transfer mechanism.

Hatami, M., et al. [51] studied the one and two-dimensional heat wave propagation in a medium subjected to different boundary conditions and with temperature dependent thermal conductivity. The effect of various parameters on the temperature distribution of the medium is analyzed by a new technique called the differential quadrature method (DQM), which provides superior results than usual FEM.

Saedodin and Torabi [52] investigated the new technique for the analytical solution of the (1+3) dimensional hyperbolic heat conduction equation (HHCE) in a cuboid solid under the space-

dependent heat flux boundary condition by separation of variables method. Four different examples were analyzed, and it was found that the new method gives similar results to the earlier investigations. Mishra and Sahai [53] used the Lattice Boltzmann method (LBM) to solve the non-Fourier heat conduction equation in 1-D cylindrical and spherical geometry. The evolution of thermal wave fronts at different time levels, including the steady state, was considered when thermal boundaries were perturbed. The LBM results were compared and found to be in good agreement with the available literature.

Kundu and Lee [54] presented the analytical work by considering the Fourier and non-Fourier heat conduction in the absorber plates of a flat-plate solar collector. The temperature shock was created with a variation of Vernotte number, and it found that the temperature response in the non-Fourier model depends on the condition of boundaries. The results show that the thermal shock wave is mainly due to isothermal boundaries, and convected boundary condition does not provide the temperature shock in the absorber plate. Zhang and Shang [55] also presented an analytical solution to non-Fourier heat conduction in a semi-infinite medium when a laser beam irradiates on its local surface. A new analytical method called Laplace and Hankel transform was used to deal with a mathematical model based on a hyperbolic heat conduction equation with thermal relaxation time. The study of the non-Fourier effect of heat propagation reveals the evaluation of the temperature field counter over time for different thermal relaxation times.

Ahmadikia and Rismanian [14] analytically studied the Fourier and hyperbolic heat transfer models subjected to periodic boundary conditions by using Laplace transform method. The thermal shock was generated at the base of the fin, which moves towards the tip of the fin and is reflected from the tip. The study on various parameters of the thermal shock location shows that relaxation time greatly influences the temperature distribution on the fin.

A one-dimensional heat conduction equation, an ordinary differential equation of second order with variable coefficients, governs the temperature variation along a rectangular annular fin. The dimensionless version of this equation is called the modified Bessel equation of zero order [18]. Initially, Harper and Brown [56] and later on other researchers [57] developed the exact analytical solution for one-dimensional heat conduction equation using the modified Bessel function of the first and second kind. In the past several exact and approximate analytical solutions have been provided by Lau and Tan [58] and by Gardner[59]. The fin optimization technique for different fins was studied by several authors and represented papers are those of Yu and Chen [60], Kundu and Das [61], Hegg and Ooi [62] and recently by Das and Kundu [63]. Other important numerical investigations also were conducted by [6],[35],[64–67]

In this study, an analytical technique called separations of variables is effectively used in the analysis of the effect of condensation on transient heat transfer on wet fins considering the dehumidifying effects. These simple analytical tools used for the heat transfer analysis were very useful and gave excellent results in line with the other techniques adopted by researchers.

2.5 Research Gap

From the above-detailed literature survey, it is evident that many researchers have analyzed the heat and mass transfer phenomena in wet fins with respect to their geometry, efficiency, and performance. But interestingly, only a few researchers concentrated on the transient thermal analysis of wet fins, considering both the Fourier and non-Fourier heat transfer modes. The transient response always exists during the initial stage of heat conduction, irrespective of fin geometry and its surface conditions. Recently, Wankhade et al. [61] analyzed the establishment of a non-Fourier heat conduction model for an accurate transient thermal response in longitudinal and pin fins. Kundu et al.[68] also suggested a unique fin design arrangement aspect to enhance the heat transfer rate under transient response on wet pin fins. Fourier and non-Fourier heat transfer model was discussed and analyzed in both studies.

While referring to the recent research works and publications by various researchers in the last five to six years, some authors have studied Fourier and Non-Fourier heat transfer models using different analytical techniques and boundary conditions related to the fin heat transfer. Hence, reviewing these published works is desirable while concluding the vast literature survey in this chapter.

In 2018, an analytical solution of Fourier and non-Fourier heat transfer in longitudinal fin with internal heat generation and periodic boundary conditions was studied by Singh et al. [72]. The study used the Laplace transform technique to include rare boundary conditions with dimensionless mathematical form. The parabolic and hyperbolic longitudinal fin models were studied. It was concluded that Fourier and non-Fourier heat conduction models showed the

same behavior without the involvement of thermal relaxation time. Also, the cooling process is faster in the non-Fourier model compared to the Fourier heat conduction model. Oguntala et al. [73] studied a numerical analysis of the transient response of a convective–radiative cooling fin with a convective tip under a magnetic field imposed for reliable thermal management of an electric system using the finite volume method. The effects of the convective tip on the thermal performance of fin were investigated. The authors pointed out that the assumption of negligible heat transfer at the fin tip is highly accurate but limited to short fins and under steady state and may not apply to the long cooling fin of finite length operating in transient heat transfer for a short time duration, which is helpful for practical implications in the design of thermally – enhanced heatsinks of solid fin under various thermal and fin tip conditions.

In 2019, Ndlovu et al. [74] analyzed the radial moving fins for temperature distribution with temperature-dependent thermal conductivity and heat transfer coefficient. The fins of hyperbolic and rectangular profiles were used for thermal behaviors, and a closed-form solution was obtained by applying the Variational Iteration Method for the convective heat transfer model. This study concluded that the heat transfer rate to the ambient fluid increases with an increase in the horizontal flow field induced by the moving fin. Oguntala et al. [75] presented a transient thermal analysis and optimization of convective–radiative porous fin under the influence of the magnetic field for efficient microprocessor cooling. This approach is crucial in the electronic industry, where small and micro-size processors are in demand, and efficient heat transfer analysis becomes a milestone. The particle swarm optimization technique was used with the finite Volume method to optimize key fin performance parameters. The study confirmed that an increase in the thermal conductivity parameter enhances heat transfer from the base of the fin to its tip, which is influenced by the radiative diffusion process.

In 2020, Some critical numerical studies by Kheirandish et al. [76] and simulation by Liu et al. [77] were also noted for the work considered non-Fourier and Fourier fin heat transfer models.

The earlier model conducted a numerical study into the fin performance subjected to different periodic base temperatures employing Fourier and non-Fourier heat conduction models and pointed out that both Fourier and non-Fourier models result in the same time-averaged fin efficiency at low disturbance amplitudes. In contrast, non-Fourier models lead to higher time-averaged fin efficiency at high disturbance amplitudes. Using the lattice Boltzmann method, the later model performed a numerical simulation of the non-Fourier heat conduction in fins. This study dealt with the heat transfer in microelectronic elements. With the high heat generation rate, the Fourier heat conduction law may not be valid, and the non-Fourier effect must be considered while designing fins in such operations. The study evaluated a non-Fourier model heat conduction and used LBM to solve thermal wave equations. Effects of thermal relaxation time, fin shape, and the frequency of the fin base temperature oscillations on the heat transfer efficiency was analyzed.

In 2021, Das and Kundu [78] investigated the simultaneous estimation of heat generation and magnetic field in a radial porous fin from surface temperature information. They highlighted that magnetic strength and heat generation always vary linearly for a given temperature distribution in fins. Kundu and Yook [79] attempted an accurate approach to thermal analysis of porous fins of different geometries with all non-linearity effects. Longitudinal, spine and radial fins were used for thermal analysis using the differential transform method to solve nonlinear equations. Fin internal heat generation and convection and radiation energy transfer with moving fin conditions were observed, and it concluded that a porous fin may be better than a solid fin depending upon the value of natural convection parameters and porosity involved in the fin design application.

In 2022, researchers [80] continued their efforts to enhance heat transfer from tall fins with cycloid thermosiphon loops. Still, some works investigated the fin efficiency of porous fins with wet surfaces [81].

In 2023, Kundu and Yook [82] presented an analytical model for extremum analysis of moistened fins involving all nonlinear energy exchange processes using ADM to predict the heat transfer duty from a moistened fin with all heat transfer modes. Some non-Fourier heat transfer models included heat transfer analysis in a longitudinal porous trapezoidal fin using an artificial neural network that was investigated by Goud et al. [83]. Gamaoun et al. [84] used a moving longitudinal radiative-convective dovetail fin for non-Fourier heat transfer analysis. They used the Cattaneo-Vernotte heat model for conduction behavioral patterns to estimate the temperature distribution in the dovetail-shaped fin. Finally, they concluded that the temperature drops from the fin's base to its tip occurred with the Fourier effect. The temperature changes rapidly at a point on the fin compared to the surroundings, and this variation remains constant for the rest of the fin.

In the above literature survey, many researchers have analyzed the fins concerning their geometry, efficiency, and performance with heat and mass transfer phenomenon. The boundary conditions, such as constant fin base temperature and isothermal fin tip condition, are adopted to simplify the thermal analysis, which is just a hypothesis in practical applications.

2.6 Objective of the thesis

A detailed literature survey shows that many researchers have analyzed wet fins' heat and mass transfer phenomena concerning their geometry, efficiency, and performance. But interestingly, only a few researchers concentrated on the transient thermal analysis of wet fins, considering both the Fourier and non-Fourier heat transfer modes.

The main objective of this paper is to analyze and highlight the effect of condensation in transient heat transfer analysis in wet fins simultaneous with dehumidifying conditions operating at a normally low-temperature range. An analytical technique called separations of variables is used effectively to calculate the temperature distribution along the fin surface of various geometries. The above literature shows that the researchers have yet to consider the rectangular and pin fin simultaneously for transient heat transfer response analysis in heat and mass transfer applications.

Further in this study, the author attempted the new fin problem, which addresses the non-Fourier heat transfer on the wet surface of the longitudinal and pin fins. In the proposed novel fin design arrangement, the fin tips are attached to primary surfaces at both ends, called fin bases. The fluid continuously passes over these primary surfaces at different temperatures, hollow or rigid in sections. The effects of wet fin surface, Fourier, and Vernotte numbers on the fin performance are also examined. Thus, this is a revolutionary attempt to provide a new fin design arrangement that is compact and reduces overall manufacturing costs.

CHAPTER-3

Establishment of non- Fourier heat conduction model for the transient thermal response in wet fins.

3.1 Introduction

In the present chapter, efforts establish a non-Fourier heat conduction model for an accurate transient thermal response in wet fins. An analytical tool called the separation of variables sets a classical analytical model defining the unsteady thermal response. The main objective of the analysis focuses on two different geometries of fins, longitudinal and pin fin, under isothermal and convective base conditions under the effect of condensation. In finned heat transfer, a transient response always exists during the initial operation of the system, like electronic cooling, nuclear reactors, and high-speed aircraft. This analysis also covers the fins used in evaporative coils used in refrigeration and air conditioning applications where the moisture in the air condenses because the fin surface temperature is below the dew point of the temperature of the surrounding humid air, which is to be cooled.

During the analysis, the instantaneous efficiency of the fin has also been calculated for both Fourier and non-Fourier heat conduction models operating under dehumidifying conditions. The results show a significant deviation in temperature response with the non-Fourier heat conduction compared to the Fourier model. Also, the effect of different design variables on transient temperature response and fin surface conditions is reported in the study. Lastly, it concludes that the instantaneous fin efficiency for the wet fin surface is always less than the

dry fin surface as the condensation on the fin surface amplifies the non-Fourier heat conduction. Hence, this non-Fourier heat transfer analysis for determining the performance parameters of wet fins would help to determine generalized design pieces of information under transient behavior conditions because it provides both Fourier and non-Fourier systems of analysis.

3.2 Mathematical formulations

The Fourier and non-Fourier effects on heat conduction under dehumidifying conditions on the fin surface are investigated in the present work. The method of separation of variables is used for the temperature distribution for the situation above. Fig. 1 shows the schematic diagram of a longitudinal and pin fin with semi-thickness, t , and length, L .

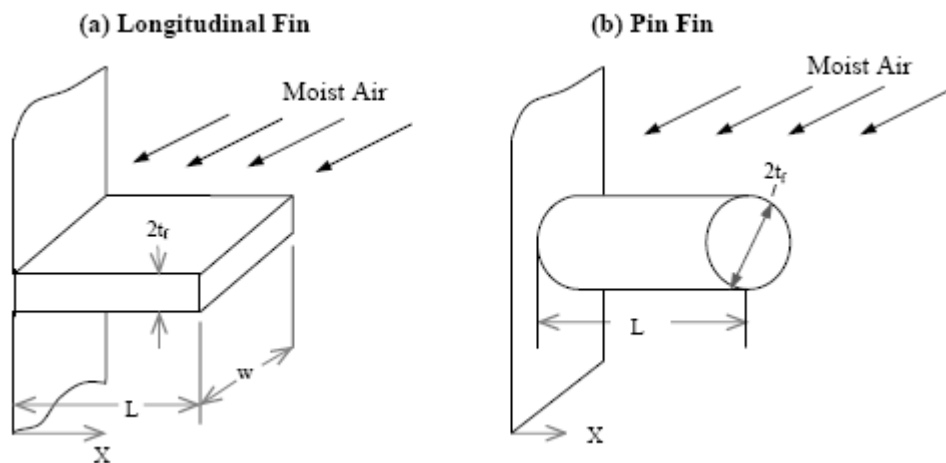


Fig. 3.1 Schematic diagram of fins.

Two types of boundary conditions are adopted to analyze the effect of non-Fourier heat conduction on temperature distribution on the fin surface. For one-dimensional transient heat transfer under dehumidifying conditions, the governing non-Fourier heat conduction equation with constant heat transfer coefficient has been taken from the law of conservation of energy used in references [35,8,17] as given below:

$$\frac{\partial^2 T}{\partial x^2} + \frac{Ph}{kA_c}(T_\infty - T) + \frac{ph_m}{kA_c}(\omega_\alpha - \omega)h_{fg} = \frac{\rho c_p}{k} \frac{\partial T}{\partial t} + \frac{\tau_r \rho c_p}{k} \frac{\partial^2 T}{\partial t^2} \quad (3.1)$$

where, T , τ_r and T_∞ are local fin surface temperature, thermal relaxation time and ambient temperature respectively. The terms, X , p , h , k , A_c represents dimensionless coordinate, fin perimeter, convection heat transfer coefficient, thermal conductivity of the fin material and fin cross section area respectively. Whereas, h_m , ω_∞ , ω , h_{fg} , ρ , and c_p signify mass transfer coefficient, specific humidity of surrounding air, specific humidity of saturated air adjacent to the fin surface, latent heat of condensation of moisture, density of fin material, and specific heat, respectively. It notes that the Fourier's law of heat conduction is a hypothesis and incompatible with the theory of relativity for considering the infinite speed of heat wave propagation within the continuum field. To encounter this contradiction, the thermal relaxation time is introduced in the heat flux expression assuming finite speed of heat wave propagation.

The ratio of fin perimeter to cross section area is expressed for longitudinal and pin fins as,

$$\frac{p}{A_c} = \frac{2(2-n)}{W} + \frac{n}{t_f} \quad (3.2)$$

The variable n equals to 1 and 2 represents the longitudinal and pin fin geometries respectively.

The Eq. (3.1) can be reduce to dimensionless form using the Chilton-Colburn relationship between heat and mass transfer coefficients [47] as,

$$\frac{\partial^2 \theta}{\partial X^2} - m^2 \left[\theta(1 + B\zeta) + \frac{C_o \zeta}{T_\infty - T_r} \right] = \frac{\partial \theta}{\partial \tau} + Ve^2 \frac{\partial^2 \theta}{\partial \tau^2} \quad (3.3)$$

where,

$$\theta = \frac{T_\infty - T}{T_\infty - T_b}; \quad X = \frac{x}{L}; \quad \frac{h}{h_m} = C_p L_e^{2/3}; \quad C_0 = \omega_a - A - BT_\alpha; \quad \zeta = \frac{h_{fg}}{C_p L_e^{2/3}}; \quad m^2 = \frac{phL^2}{kA_c}$$

$$\tau = \frac{\alpha t}{L^2}; \quad Ve^2 = \frac{\tau_r \alpha}{L^2} \quad (3.4)$$

This Eq. (3.4) can be further reduced and simplified as,

$$\frac{\partial^2 \phi}{\partial X^2} - Z_0^2 \phi = \frac{\partial \phi}{\partial \tau} + Ve^2 \frac{\partial^2 \phi}{\partial \tau^2} \quad (3.5)$$

where,

$$Z_0^2 = [2(2-n)t^* + n] \frac{Bi}{\psi^2} (1 + B\zeta); \quad \phi = \theta + \theta_p;$$

$$t^* = \frac{t_f}{W}; \quad Bi = \frac{ht_f}{k}; \quad \psi = \frac{t_f}{L}; \quad \theta_p = \frac{C_0 \zeta}{(T_\infty - T_r)(1 + B\zeta)} \quad (3.6)$$

Eq. (3.5) has been derived based on the assumption of constant thermo-physical properties applied to the heat flow, which is a well-justified assumption. For example, the thermal conductivity of fin material has been considered a constant as there is a slight temperature variational range in wet fins for refrigeration and air conditioning applications. Hence, the influence of temperature on thermal conductivity is assumed as constant in this study.

Eq. (3.5) demonstrates the non-Fourier heat transfer in wet fins. It becomes the governing equation for Fourier heat conduction in fins if, the Vernotte number, Ve , vanishes and can be expressed as,

$$\frac{\partial^2 \phi}{\partial X^2} - Z_0^2 \phi = \frac{\partial \phi}{\partial \tau} \quad (3.7)$$

Two boundary conditions associated with the fin base and fin tip were considered for one-dimensional heat conduction in the fin. Usually, to simplify the analysis, the fin base

temperature is assumed constant, and the fin tip is to be insulated. However, heat transfer due to convection is possible at these two ends. Possible practical initial and boundary conditions are used for the solution of Eq. (3.5) with a non-Fourier heat condition model and expressed mathematically as,

Initial Condition:

$$\text{at } \tau = 0 \quad (0 \leq X \leq 1), \quad \phi(X, \tau) = \theta_p \quad (3.7a)$$

$$\text{at } \tau = 0 \quad (0 \leq X \leq 1), \quad \frac{\partial \phi(X, \tau)}{\partial \tau} = 0 \quad (3.7b)$$

Boundary conditions: ($\tau > 0$)

$$\text{at } X = 0$$

$$\left\{ \begin{array}{ll} \phi(X, \tau) = 1 + \theta_p & \text{(Constant base temperature),} \\ \frac{\partial \phi(X, \tau)}{\partial X} + Bi_0 \phi(X, \tau) - Bi_0 (1 + \theta_p) = 0 & \text{(Convected base condition)} \end{array} \right. \quad (3.7c)$$

$$\text{at } X = 1, \quad \frac{\partial \phi(X, \tau)}{\partial X} = -Bi_t (1 + B\zeta) \phi(X, \tau) \quad (3.7d)$$

where, $Bi_0 = \frac{h_L L}{k}$ and $Bi_t = \frac{h_t L}{k}$. Amongst these two Biot numbers, the Biot number based

on the fin base condition Bi_0 , is always greater than the Biot number based on the fin tip condition Bi_t for the heat transfer from primary surface to surrounding. Eq. (3.7) with the boundary conditions given by Eqs. (3.7a), (3.7c), and (3.7d) can be used for Fourier heat conduction analysis for comparison between Fourier and non-Fourier analysis. Some boundary and initial conditions are homogeneous for solving the heat conduction equation. Many researchers, especially [54-59] have conducted extensive studies on heat transfer and fluid flow

problems in recent years. However, in the present chapter, the separation of variables is employed for Eq. (3.5) to obtain an exact analytical solution. Eq. (3.5) involves non-Fourier heat conduction and initially requires converting homogeneous equations using new variables as,

$$\phi(X, \tau) = \Gamma(X) + \Omega(X, \tau) \quad (3.8)$$

Eq.(3.5) can be formulated by using Eq.(3.8) as,

$$\frac{d^2\Gamma}{dX^2} - Z_0^2\Gamma = 0 \quad (3.9a)$$

and

$$\frac{\partial^2\Omega}{\partial X^2} - Z_0^2\Omega = Ve^2 \frac{\partial^2\Omega}{\partial \tau^2} + \frac{\partial\Omega}{\partial \tau} \quad (3.9b)$$

For finding the solution of equation (3.9), the initial and boundary conditions are obtained by combining Eqs. (3.7) and (3.8) as,

$$\text{at } \tau = 0 \quad (0 \leq X \leq 1), \quad \Gamma(X) + \Omega(X, \tau) = \theta_p \quad (3.10a)$$

$$\text{at } \tau = 0 \quad (0 \leq X \leq 1), \quad \frac{\partial\Omega(X, \tau)}{\partial \tau} = 0 \quad (3.10b)$$

$$\text{at } X = 0 \quad (\tau > 0) \quad \Gamma(X) = 1 + \theta_p \quad \text{and} \quad \Omega(X, \tau) = 0 \quad (\text{Constant base temperature}) \quad (3.10c)$$

$$\text{at } X = 0 \quad (\tau > 0),$$

$$\left\{ \begin{array}{l} \frac{\partial\Omega(X, \tau)}{\partial X} + Bi_o\Omega(X, \tau) = 0 \\ \frac{d\Gamma(X)}{dX} + Bi_o\Gamma(X) + Bi_o(1 + \theta_p) = 0 \end{array} \right. \quad (\text{Convected base condition}) \quad (3.10d)$$

$$\text{at } X = 0 \quad (\tau > 0),$$

$$\left\{ \begin{array}{l} \frac{\partial\Omega(X, \tau)}{\partial X} + Bi_i(1 + B\zeta)\Omega = 0 \\ \frac{d\Gamma(X)}{dX} + Bi_i(1 + B\zeta)\Gamma(X) = 0 \end{array} \right. \quad (3.10e)$$

From the above boundary conditions, it can be said that, at the base, two boundary conditions are used for the present analysis. The fin tip undergoes heat transfer due to convection with a heat transfer coefficient. The insulated tip condition may be selected by assigning a zero value for the heat transfer coefficient at the fin tip. The solution of Eq. (3.9a) for both the base conditions can be expressed as,

For constant base temperature,

$$\Gamma(X) = (1 + \theta_p) \left\{ \frac{Z_0 \cosh[Z_0(1-X)] + Bi_t(1+B\zeta) \sinh[Z_0(1-X)]}{Z_0 \cosh Z_0 + Bi_t(1+B\zeta) \sinh Z_0} \right\} \quad (3.11a)$$

and

for convected base condition,

$$\Gamma(X) = (1 + \theta_p) Bi_0 \left\{ \frac{\cosh[Z_0(1-X)] + A_3 Bi_0 \sinh[Z_0(1-X)]}{A_1 \cosh Z_0 + A_2 \sinh Z_0} \right\}, \quad (3.11b)$$

where,

$$A_1 = Bi_0 + Bi_t(1+B\zeta) \quad (3.12a)$$

$$A_2 = Z_0 + Bi_0 Bi_t(1+B\zeta) \quad (3.12b)$$

and

$$A_3 = Bi_t(1+B\zeta) \cdot Z_0^{-1} \quad (3.12c)$$

Eq.(3.9b) can be solved by using the product method. For this methodology, it is assumed that,

$$\Omega(X, \tau) = A(X) B(\tau) \quad (3.13)$$

Using the above relationship, Eqs. (3.9b) and (3.10) can be expressed by adopting the separation of the two variables as mentioned below,

$$\frac{\partial^2 A(X)}{\partial X^2} + \lambda^2 A(X) = 0 \quad (3.14a)$$

$$Ve^2 \frac{\partial^2 B(\tau)}{\partial \tau^2} + \frac{\partial B(\tau)}{\partial \tau} + (Z_0^2 + \lambda^2) B(\tau) = 0 \quad (3.14b)$$

$$A(X) B(0) + \Gamma(X) = \theta_p \quad (3.14c)$$

$$\frac{dB(0)}{d\tau} = 0 \quad (3.14d)$$

$$A(0) = 0 \quad (\text{Constant base temperature}) \quad (3.14e)$$

$$\frac{dA(0)}{dX} + Bi_0 A(0) = 0 \quad (\text{Convected base}) \quad (3.14f)$$

and

$$\frac{dA(1)}{dX} + Bi_t (1 + B\zeta) A(1) = 0 \quad (3.14g)$$

From Eqs. (3.14a), (3.14e) and (3.14g), the following relationship can be obtained:

$$\lambda_n = \alpha_n + (2n+1)\pi/2 \quad \text{for } n = 0, 1, 2, \dots \quad (3.15a)$$

where,

$$\alpha_n = \tan^{-1} \left[\frac{Bi_t (1 + B\zeta)}{\lambda_n} \right] \quad (3.15b)$$

After combining equations (3.14a), (3.14f) and (3.14g) yields to,

$$\lambda_n - \beta_n = n\pi \quad \text{for } n = 0, 1, 2, \dots \quad (3.16a)$$

where,

$$\tan \beta_n = \frac{\lambda_n [Bi_0 + Bi_t (1 + B\zeta)]}{\lambda_n^2 Bi_0 Bi_t (1 + B\zeta)} \quad (3.16b)$$

Eigen values λ_n are determined using Eqs. (3.15) and (3.16). Newton-Raphson iterative

method has been employed here to solve these transcendental equations. From Eqs. (3.11) and

(3.14), $\phi(X, \tau)$ can then be determined considering the constant base temperature and convected base condition, respectively and expressed as,

$$\phi(X, \tau) = \frac{(1 + \theta_p)}{\Gamma_1} [Z_0 \cosh\{Z_0(1 - X)\} + Bi_t(1 + B\zeta)\sinh\{Z_0(1 - X)\}] + \begin{cases} \sum_{n=0}^{\infty} (D_2 - D_1)^{-1} I_n [D_2 \exp(D_1 \tau) - D_1 \exp(D_2 \tau)]; & \text{for } 1 - 4V_e^2(Z_0^2 + \lambda_n^2) > 0 \\ \sum_{n=0}^{\infty} (1 - D_0 \tau) I_n \exp(D_0 \tau); & \text{for } 1 - 4V_e^2(Z_0^2 + \lambda_n^2) = 0 \\ \sum_{n=0}^{\infty} E_0^{-1} I_n \exp(D_0 \tau) [E_0 \cos(E_0 \tau) - D_0 \sin(E_0 \tau)]; & \text{for } 1 - 4V_e^2(Z_0^2 + \lambda_n^2) < 0 \end{cases} \quad (3.17a)$$

$$\phi(X, \tau) = (1 + \theta_p) Bi_0 \left\{ \frac{\cosh[Z_0(1 - X)] + A_3 Bi_0 \sinh[Z_0(1 - X)]}{A_1 \cosh Z_0 + A_2 \sinh Z_0} \right\} + \begin{cases} \sum_{n=0}^{\infty} (D_2 - D_1)^{-1} J_n [D_2 \exp(D_1 \tau) - D_1 \exp(D_2 \tau)]; & \text{for } 1 - 4V_e^2(Z_0^2 + \lambda_n^2) > 0 \\ \sum_{n=0}^{\infty} (1 - D_0 \tau) J_n \exp(D_0 \tau); & \text{for } 1 - 4V_e^2(Z_0^2 + \lambda_n^2) = 0 \\ \sum_{n=0}^{\infty} E_0^{-1} J_n \exp(D_0 \tau) [E_0 \cos(E_0 \tau) - D_0 \sin(E_0 \tau)]; & \text{for } 1 - 4V_e^2(Z_0^2 + \lambda_n^2) < 0 \end{cases} \quad (3.17b)$$

where,

$$(D_1, D_2) = \frac{-1 \pm \sqrt{1 - 4V_e^2(Z_0^2 + \lambda_n^2)}}{2V_e^2} \quad (3.18a)$$

$$D_0 = (-1/2V_e^2) \quad (3.18b)$$

$$E_0 = \frac{\sqrt{4V_e^2(Z_0^2 + \lambda_n^2) - 1}}{2V_e^2} \quad (3.18c)$$

$$I_n = \frac{4\lambda_n \sin(\lambda_n X)}{[2\lambda_n - \sin(2\lambda_n)]} \left[\frac{\theta_p}{\lambda_n} (1 - \cos \lambda_n) - \frac{(1 - \theta_p) Z_0 \lambda_n}{\Gamma_1 (\lambda_n^2 + Z_0^2)} (\cosh Z_0 - \cos \lambda_n) - \frac{Bi_t (1 + \theta_p) (1 + B\zeta)}{\Gamma_1 (\lambda_n^2 + Z_0^2)} (\lambda_n \sinh Z_0 - Z_0 \sin \lambda_n) \right] \quad (3.18d)$$

$$J_n = \frac{4\lambda_n \cos(\gamma_n - \lambda_n X)}{[2\lambda_n - \sin(2\gamma_n) - \sin(2\gamma_n - 2\lambda_n)]} \left[\begin{array}{l} \frac{\theta_p}{\lambda_n} \{ \sin \gamma_n - \sin(\gamma_n - \lambda_n) \} - \frac{(1 + \theta_p) Bi_0}{\Gamma_2 (\lambda_n^2 + Z_0^2)} \\ \times \{ \lambda_n \cosh Z_0 \sin \gamma_n + Z_0 \sinh Z_0 \cos \gamma_n - \lambda_n \sin(\gamma_n - \lambda_n) \} \\ - \frac{Bi_t Bi_0 (1 + \theta_p) (1 + B\zeta)}{\Gamma_2 (\lambda_n^2 + Z_0^2) Z_0} \\ \times \{ \lambda_n \sinh Z_0 \sin \gamma_n + Z_0 \cosh Z_0 \cos \lambda_n - Z_0 \cos(\gamma_n - \lambda_n) \} \end{array} \right] \quad (3.18e)$$

where,

$$\Gamma_1 = (Z_0) \cosh(Z_0) + Bi_t (1 + B\zeta) \sinh(Z_0) \quad (3.18f)$$

and

$$\Gamma_2 = A_1 \cosh(Z_0) + A_2 \sinh(Z_0) \quad (3.18g)$$

Considering the Fourier heat transfer model, the following temperature distribution can be obtained from Eqs. (3.7), (3.7a), (3.7c), and (3.7d) for the constant base temperature and the convected base conditions, respectively, as,

$$\begin{aligned} \phi(X, \tau) = & \frac{(1 + \theta_p)}{\Gamma_1} [Z_0 \cosh\{Z_0(1 - X)\} + Bi_t (1 + B\zeta) \sinh\{Z_0(1 - X)\}] \\ & + \sum_{n=0}^{\infty} \frac{4\lambda_n e^{-(\lambda_n^2 + Z_0^2)\tau} \cdot \sin(\lambda_n X)}{(2\lambda_n - \sin 2\lambda_n)} \left[\begin{array}{l} \frac{\theta_p}{\lambda_n} (1 - \cos \lambda_n) - \frac{(1 + \theta_p) Z_0 \lambda_n}{\Gamma_1 (Z_0^2 + \lambda_n^2)} (\cosh Z_0 - \cos \lambda_n) \\ - \frac{Bi_t (1 + \theta_p) (1 + B\zeta)}{\Gamma_1 (Z_0^2 + \lambda_n^2)} (\lambda_n \sinh Z_0 - Z_0 \sin \lambda_n) \end{array} \right] \end{aligned} \quad (3.19a)$$

and

$$\begin{aligned} \phi(X, \tau) = & (1 + \theta_p) Bi_0 \left\{ \frac{\cosh[Z_0(1 - X)] + A_3 \sinh[Z_0(1 - X)]}{A_1 \cosh Z_0 + A_2 \sinh Z_0} \right\} \\ & + \sum_{n=0}^{\infty} \frac{4\lambda_n \cos(\lambda_n - \lambda_n X) \exp[-\lambda_n^2 + Z_0^2]}{[2\lambda_n + \sin(2\gamma_n) - \sin(2\gamma_n - \sin 2\lambda_n)]} \\ & \times \frac{\theta_p}{\lambda_n} \{ \sin \gamma_n - \sin(\gamma_n - \lambda_n) \} - \frac{(1 + \theta_p) Bi_0}{\Gamma_2 (\lambda_n^2 + Z_0^2)} \end{aligned}$$

$$\times \{ \lambda_n \cosh Z_0 \sin \gamma_n + Z_0 \sinh Z_0 \cos \gamma_n - \lambda_n \sin(\gamma_n - \lambda_n) \} \\ - \frac{Bi_t Bi_0 (1 + \theta_p)(1 + B\zeta)}{\Gamma_2(\lambda_n^2 + Z_0^2) Z_0} \{ \lambda_n \sinh Z_0 \sin \gamma_n + Z_0 \cosh Z_0 \cos \gamma_n - Z_0 \cos(\gamma_n - \lambda_n) \} \quad (3.19b)$$

For all positive instances, the temperature in the fin varies from the fin-base to fin-tip. The mean temperature in the fin as a function of time can be obtained from Eqs. (3.17) - (3.19) as,

$$\phi_m(\tau) = \int_{X=0}^1 \phi(X, \tau) dX \quad (\tau > 0) \quad (3.20)$$

The instantaneous heat transfer rate for longitudinal and pin fin can determined using the following expression as,

$$Q = \frac{q}{2kL(T_\infty - T_r)} \\ = \pi^{m-1} (1 + B\zeta) \left[\left(3 - m + \frac{2-m}{t^*} \right) Bi \phi_m + \frac{Bi_t \psi \phi_t}{mt^{*2-m}} \right] \quad (3.21)$$

where ϕ_t is the dimensionless tip temperature which can be obtained from Eqs. (3.17) - (3.19).

The instantaneous efficiency can be expressed in the following manner,

$$\eta = \left[\frac{\left(3 - m + \frac{2-m}{t^*} \right) Bi \phi_m + \frac{Bi_t \psi \phi_t}{mt^{*2-m}}}{\left(3 - m + \frac{2-m}{t^*} \right) Bi \phi_b + \frac{Bi_t \psi \phi_b}{mt^{*2-m}}} \right] \quad (3.22)$$

where ϕ_b is the dimensionless base temperature. Here it should be noted that Eqs. (3.19) and (3.20) are infinite convergence series; hence only some terms of these infinite series may yield

high accuracy. In this study, the first hundred terms were selected to get the final results with an accuracy of eight decimal points. This type of decaying response has been investigated by a researcher[70] in the study of transient heat transfer.

3.3 Result and Discussion

The main objective of this study is to investigate the transient temperature response in wet fins considering non-Fourier heat conduction subject to different boundary conditions. Some dimensionless parameters such as Vernotte number, Fourier number, and Biot number at the fin base and fin tip were studied in the analysis. The analytical technique called separation of variables is adopted to determine the temperature distribution and fin efficiency under dehumidifying conditions for heat conduction in the fin governed by Fourier and non-Fourier laws. Some arbitrary design values based on earlier studies were considered for the analysis are, $\psi = 0.1$, $p_a = 1.013$ bar, $T_a = 30^\circ C$, $T_r = 3^\circ C$ and $RH = 100\%$. These values are not limited to this study, but it is suitable to consider any other values depending on the design requirement. Furthermore, the design constants should be selected to satisfy the one-dimensional heat flow and fully wet fin surface conditions. However, all these design variables except ψ are not required for dry fin surface analysis.

3.4 Validation of the present research work

The mathematical analysis developed in this study has been validated before presenting the results. The validation is done by deriving the steady-state temperature distribution in the wet

fin from (Eq. 3.5) along with the boundary conditions taken as expressed in Eqs. (3.7c) and (3.7d). The equation for the steady temperature of the wet fin for constant base temperature and the convected base condition is obtained and expressed respectively as,

$$\frac{\phi}{1+\theta_p} = \frac{Z_0 \cosh[Z_0(1-x)] + Bi_t(1+B\zeta)\sinh[Z_0(1-x)]}{Z_0 \cosh(Z_0) + Bi_t(1+B\zeta)\sinh(Z_0)} \quad (3.23a)$$

and

$$\frac{\phi}{(1+\theta_p)Bi_0} = \frac{Z_0 \cosh[Z_0(1-x)] + Bi_t(1+B\zeta)\sinh[Z_0(1-x)]}{[Z_0^2 + Bi_0Bi_t(1+B\zeta)]\sinh(Z_0) + Z_0[Bi_0 + Bi_t(1+B\zeta)]\cosh(Z_0)} \quad (3.23b)$$

Fig. 3.2 shows the dimensionless temperature ϕ as a function coordinate X at constant thermo-physical and psychrometric parameters using Eqs. (3.23a) and (3.23b). The correctness of the present model is established and the temperature response based on Fourier and non-Fourier approaches is plotted and compared in Fig. 2 at $Z_0 = 0.5$. Here it is important to note that the present transient model can be adopted for a steady model at a higher value of Fourier number,

τ .

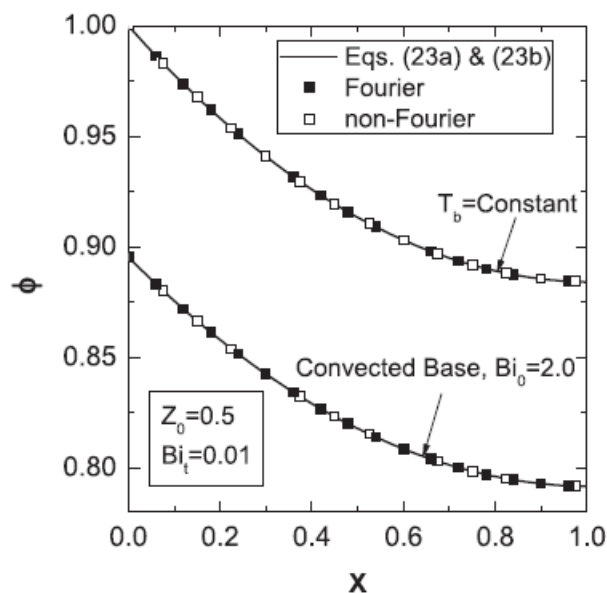


Fig. 3.2 Validation of the present study for a high value of τ with its steady condition.

It is also worth to highlight that at this high value of τ , both Fourier and non-Fourier models coincides and becomes a single model. This approach is considered for the validation and Fig. 3. 2 is plotted for $\tau = 100$ and $V_e = 2.0$ for the non-Fourier model. Though these transient parameters have been taken arbitrarily, but it should be assured at high value of τ the transient phenomena vanished. As shown in the results plotted in Fig. 3.2, it can easily be demonstrated that the present model has been correctly formulated.

Now, a numerical scheme based on the finite difference method has also been developed to validate the present methodology with the transient characteristics. For obtaining the difference equations, discretization of the governing fin equation for non-Fourier heat conduction, Taylor series-based central difference scheme with the Crank-Nicolson implicit method has been used. These difference equations are solved simultaneously at the pivotal points by using the

Gauss-Seidel iterative process after satisfying the appropriate initial and boundary conditions and convergence criterion (10^{-6}). Also, the grid independency test has been carried out. When results are taken, an insignificant variation (less than 0.1%) has been observed.

Fig.3.3 has also been drawn for the validation purpose corresponding to $V_e = 2.0$, $Bi = 0.001$, $Bi_t = 0.01$ and $Bi_0 = 2.0$. It shows the mean temperature response in fins under convective base condition with longitudinal and pin fins geometries. Here, it can be mentioned that instead of Z_0 , Bi has been considered as a design variable. It can lead to separate analyses for longitudinal and pin fins, and a comparison can be made between them. Furthermore, the selection of Bi has always provided a guideline for one-dimensional heat flow; therefore, it is important from an analysis point of view.

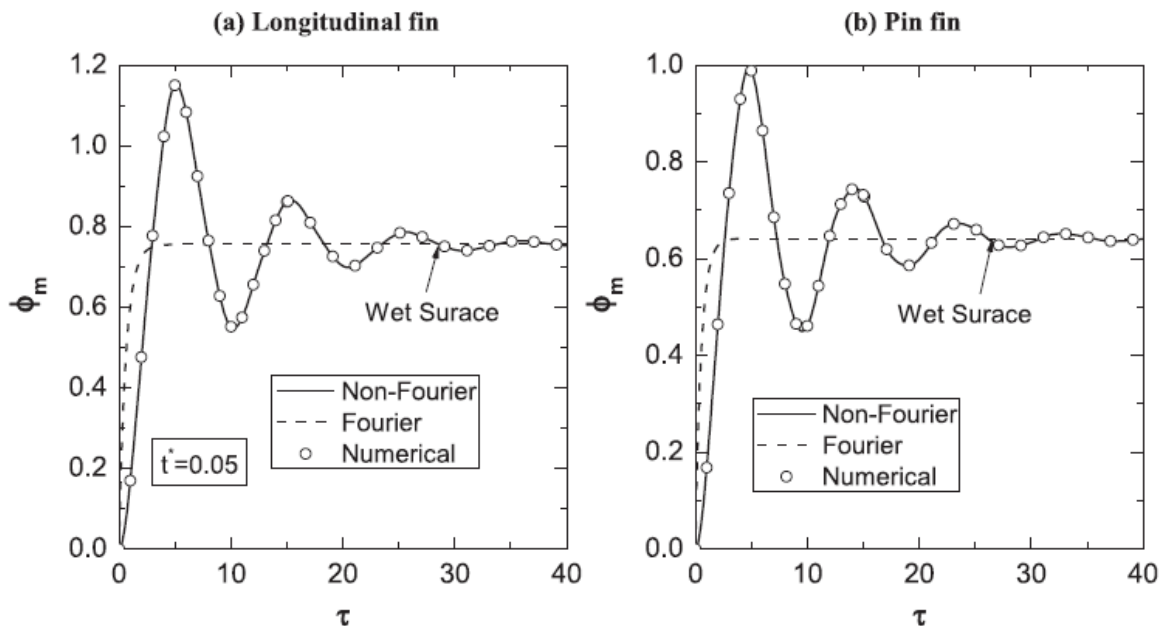


Fig. 3.3 Results obtained from the present analytical analysis and numerical analysis.

The data regarding temperature have been compared from the present analytical and numerical analysis for wet fins using non-Fourier heat conduction. From these figures, it highlights that both results presented agree. Also, the same figure compares the temperature response obtained with the non-Fourier model against the Fourier conduction model. It observes that apart from the considerable deviation of temperatures obtained with Fourier and non-Fourier models at smaller values of the Fourier number, there is no significant difference between these two models at higher values of the Fourier number.

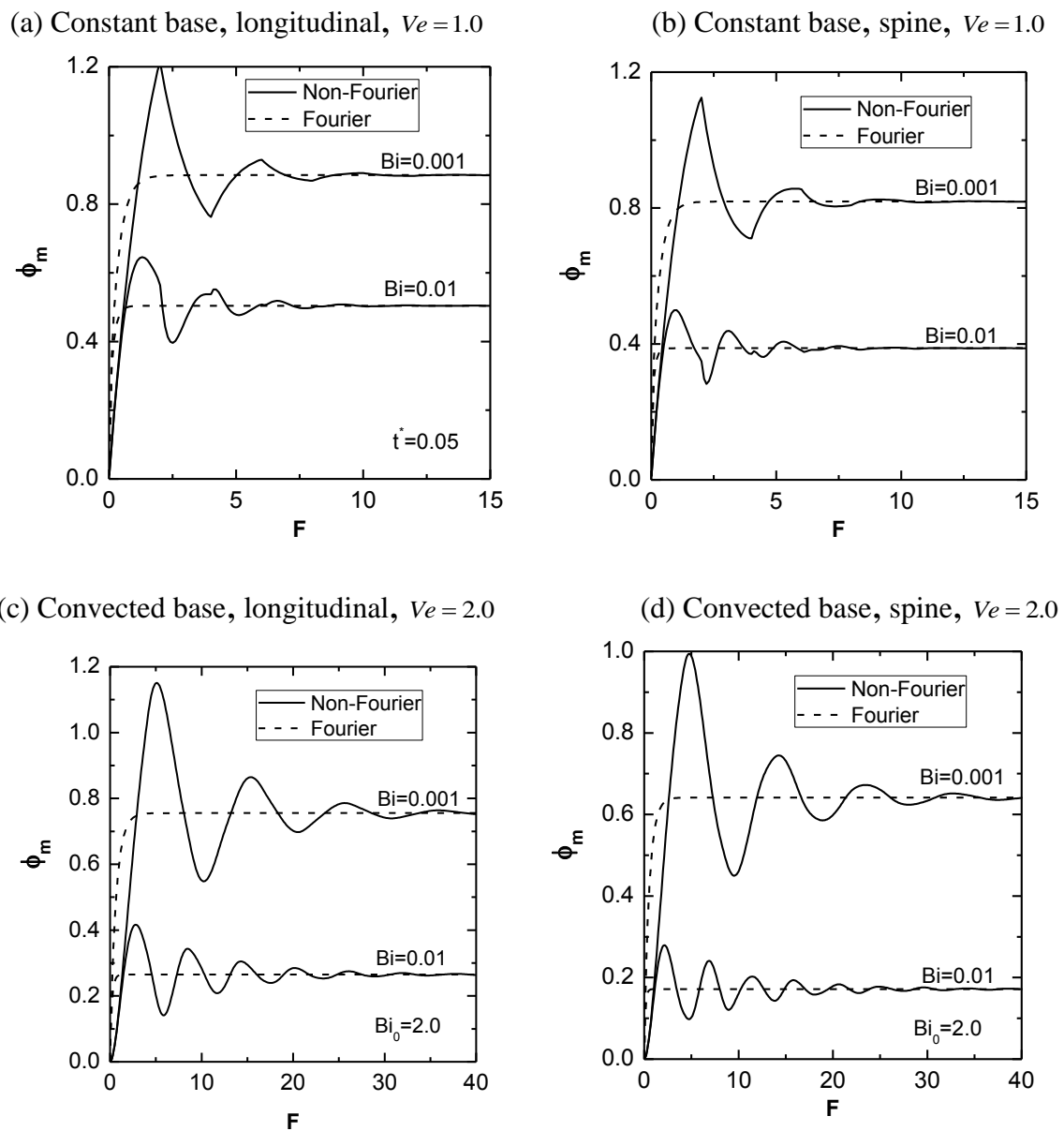


Fig. 3.4 Mean temperature in a fin as a function of Fourier and Biot numbers.

3.5 Non-Fourier heat conduction model for transient thermal response in wet fins

The significance of the non-Fourier analysis is shown with the help of Fig. 3.4, in which mean temperature in fins as a function of Fourier number is assessed using the Fourier and the non-Fourier analysis, and also the comparison is made for $Bi_i = 0.01$. This figure can easily demonstrate that, at smaller values of the Fourier number, the non-Fourier model shows more deviation than the Fourier model at different values of the Biot number, Vernotte number, and base conduction. Fig. 3.4a and 3.4b demonstrate the variation in the mean temperature of a fin with longitudinal and pin fin geometries for the non-Fourier heat conduction model at different values of the Biot number and $V_e = 1.0$ at a constant base temperature. At low values of the Biot number and Fourier number, the mean temperature distribution curve shows large amplitudes. Similarly, for greater values of Fourier number, the temperature response with both high and low Biot numbers exhibits similar behavior before the Fourier, and non-Fourier heat transfer conditions reach a steady state. Fig. 3.4c and 3.4d shows a similar pattern for mean temperature distribution in the convected base condition for $V_e = 2.0$. It is evident that at the increased value of the Vernotte number, the transient effect is more dominant. This physical effect is more prominent in the case of longitudinal fin geometry and at constant base temperature for the same Vernotte number. However, for identical Biot numbers, the variation in the mean temperature between the fin-base and the fin-tip is always higher at an isothermal base due to the base temperature possessing the highest value. It is also observed that the ripple of temperature response for the convected base is smoother compared to the isothermal base.

This is probably because of no restriction on the heat propagation within the fin material corresponding to the pertinent boundary condition. From Fig. 3.4, It can be concluded that Fourier heat transfer shows a similar trend for both the base conditions irrespective of the fin geometries. In comparison, the non-Fourier heat transfer behavior changes at different Vernotte numbers, Fourier numbers, fin geometry, and boundary conditions.

Fig. 3.5 illustrates the heat transfer rate in a fin with dry and wet surface considering both Fourier and non-Fourier heat conduction models. For constant and convected base condition, the study has been carried out for Biot number, $Bi = 0.001$, $V_e = 2.0$ and $Bi_t = 0.01$. To show the comparisons, the heat transfer obtained from the Fourier model is also plotted in Fig. 3.5. It points out that with an increasing function, the Fourier heat transfer varies against time until it reaches a steady value for both the boundary conditions considered at the fin base irrespective of the fin geometries. However, for different base boundary conditions and due to the non-Fourier heat conduction, a noticeable and pronounced effect can be seen during the transient heat transfer response in the fin. The wet fin surface under dehumidification enhances the waviness amplitude for these boundary conditions and geometries. The convective base condition shows distinctness in the magnitude of the curve compared to the constant base condition. Furthermore, the curve with the convective base condition looks smoother than the corresponding isothermal base condition.

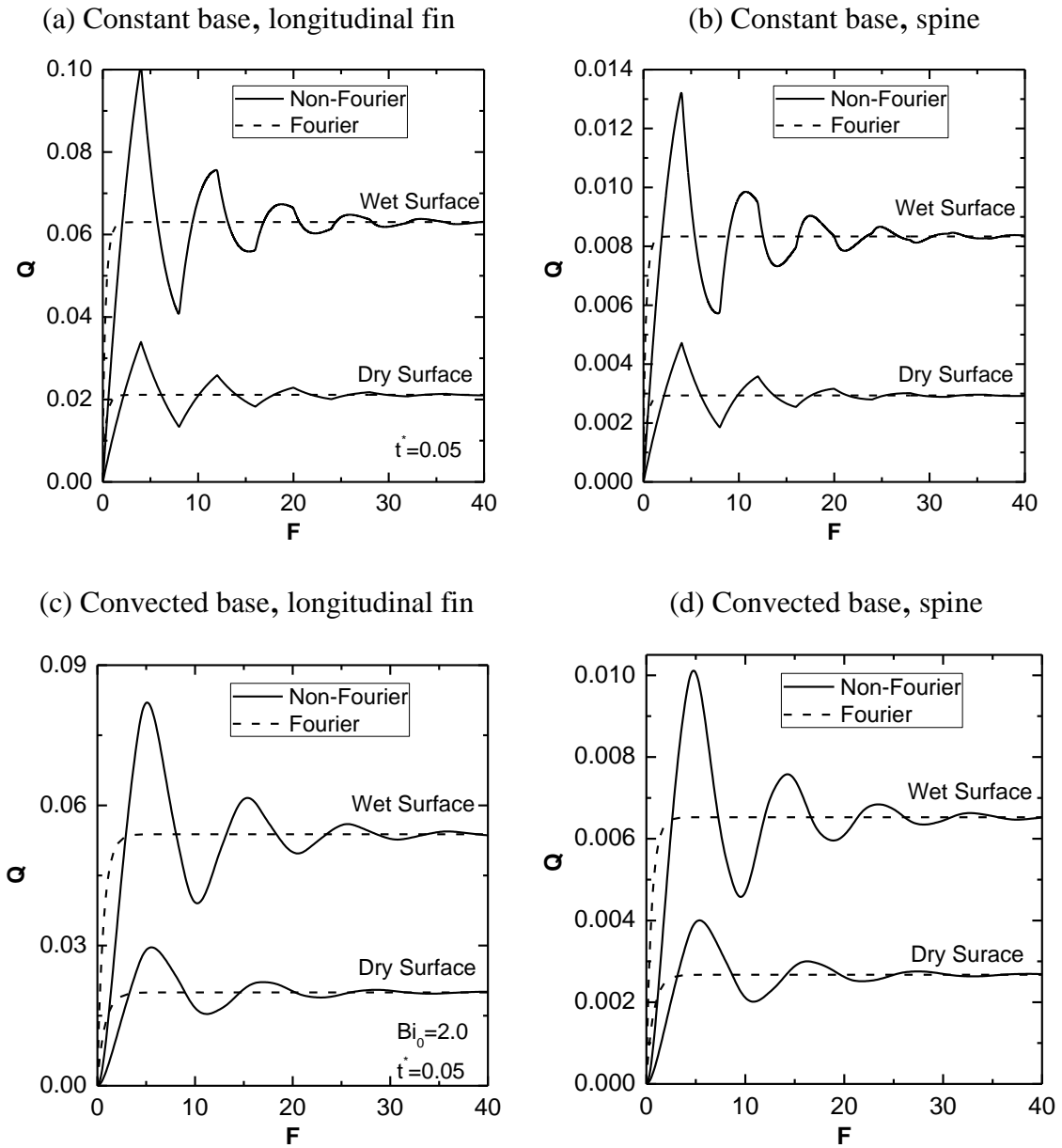


Fig. 3.5 Heat transfer in a fin for dry and wet surfaces.

The influence of the Vernotte number on the heat transfer in the wet fin can be seen in Fig. 3.6. The data shown in Fig. 3.6 and Fig. 3.5 based on the same parameters and only Ve is different. A clear and distinguishable heat transfer rate is observed in Fig. 3.6 for various values of the Vernotte number, at $Bi = 0.001$ and $Bi_t = 0.01$.

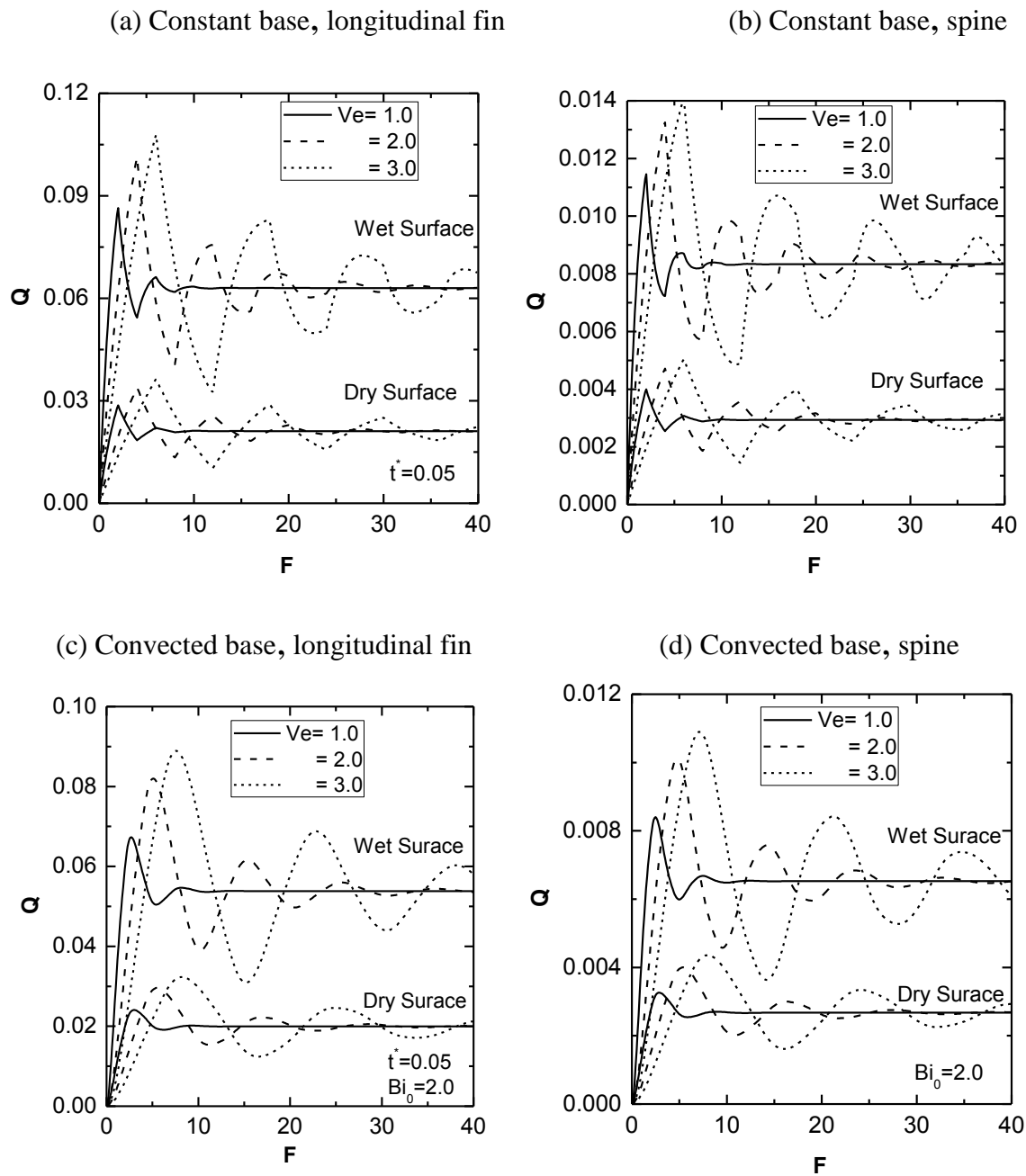


Fig. 3.6 Heat transfer as a function of Fourier and Vernetto numbers for dry and wet surfaces.

In the above case for higher values of V_e , higher amplitudes in the heat transfer rate is observed for both the base conditions. This effect can be clearly observed with variation of the fin geometry. The difference in the dry and wet surface responses to the non-Fourier heat conduction is also demonstrated in this figure and can be confirmed that it is primarily

dependent on the Fourier number. In case of wet fin surfaces, the heat transfer rate may be much more at a lower value of Fourier number. The effect of V_e and τ on the heat transfer rate in dry and wet fins can also be seen in this figure. It can be concluded that the non-Fourier effect on the heat transfer rate in wet fins is always higher than that of the dry fin. Hence, considering the non-Fourier heat transfer model is always desirable for precise design analysis of wet fins. A higher value of the Vernotte number requires more thermal relaxation time, which can be clearly seen in both the base conditions, especially for the wet fin surface in the presence of a thin film.

The variation in heat transfer rate as a function of Fourier and Vernotte number for dry and wet surfaces with tip Biot number is shown in Fig. 3.7 at $Bi = 0.001$, $V_e = 2.0$ and $\tau = 5.0$.

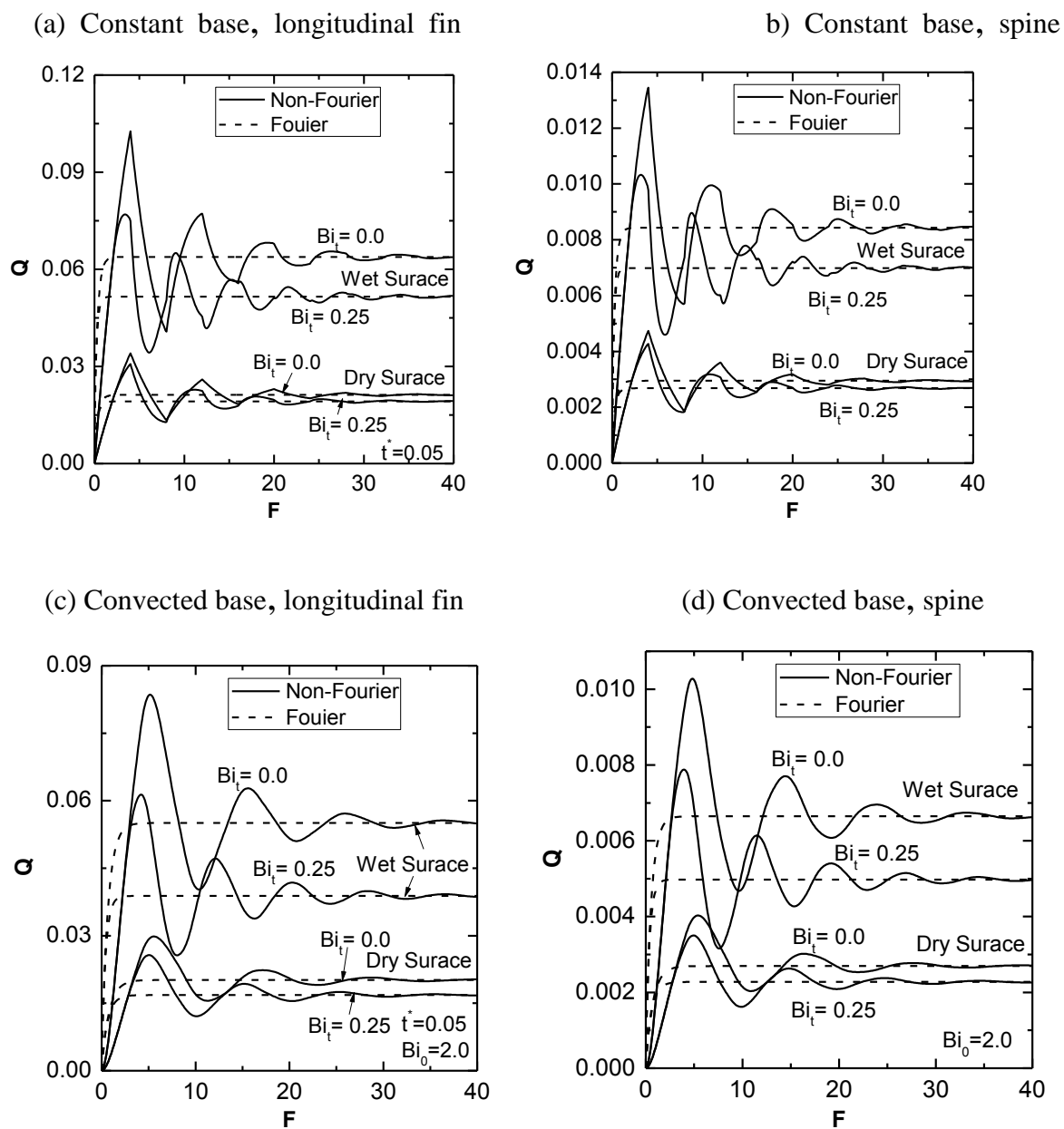


Fig. 3.7 Heat transfer as a function of Fourier number and tip Biot number for dry and wet surfaces.

For the isothermal base condition, Figs. 3.7a and 3.7b are plotted using the longitudinal and pin fin geometries, respectively. The tip Biot number does not influence the nature of Fourier heat transfer in both geometries. However, considering the non-Fourier analysis, with lower values of the Biot number, the wet fin surface exhibits more transient effects along with higher

amplitude and waviness. Fig. 3.7c and 3.7d also show identical behavior but with lesser amplitudes in the curve profile. This smoothness in the curve may be due to convective heat transfer along the base surface. The Fourier heat transfer curve depicts almost the mean heat transfer value for the base and surface conditions.

Fig.3. 8 illustrates the heat transfer and fin efficiency as a function of tip Biot number for dry and wet fin surfaces under the effect of non-Fourier heat transfer. Results have been shown for $Bi = 0.001$, $V_e = 2.0$, $\tau = 5.0$ and $Bi_0 = 2.0$. It is important to note here that, the instantaneous fin efficiency has been determined for the first time with non-Fourier heat conduction.

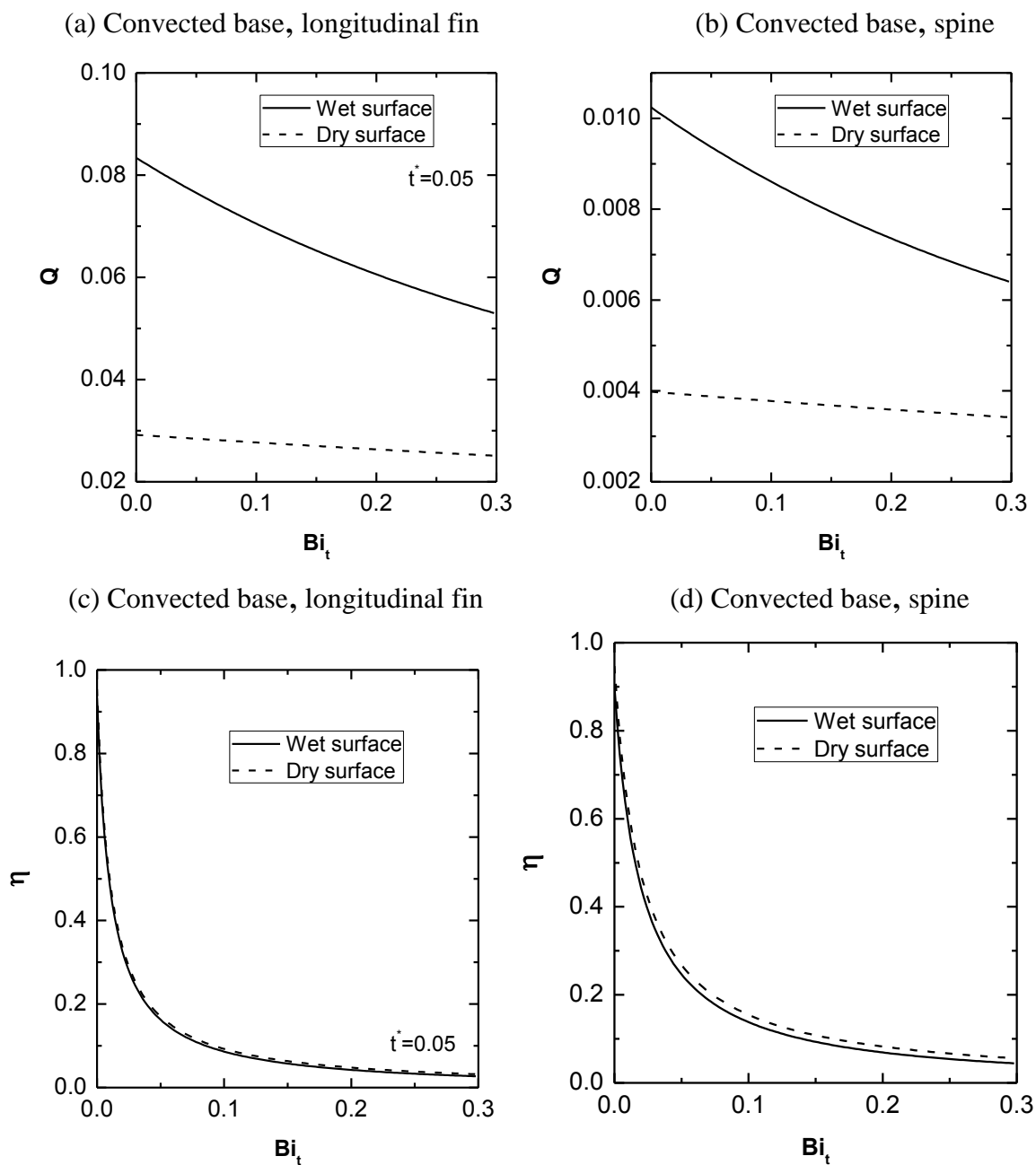


Fig. 3.8 Heat transfer and fin efficiency as a function of tip Biot number for dry and wet surfaces.

Figs. 3.8a and 3.8b show the convected base condition for both fin geometries. It is observed that the longitudinal fin with a wet surface has higher heat transfer rate values than that of the pin fin. In this regard, it can be stated that the longitudinal fin has more surface area exposed to the surrounding air. The heat transfer rate in the case of dry fin surface decreases slowly

with Bi_t and is relatively more for wet surface fins. This reduction in the heat transfer rate with Bi_t for both dry and wet surfaces is due to the decrease in temperature difference between the surrounding air and the fin surface. In Figs. 3.8c and 3.8d, it is demonstrated that the fin efficiency almost remains the same for wet and dry surface conditions in the case of the longitudinal fin. From these figures, it can be concluded that the influence of the fin efficiency on Bi_t is relatively more for spine fin geometry than the longitudinal fin.

Fig. 3.9 depicts heat transfer rate and fin efficiency as a function of base Biot number, Bi_0 for wet and dry surfaces considering non-Fourier heat conduction mode. Various parameters have been considered as $Bi = 0.001$, $V_e = 2.0$, $\tau = 5.0$ and $Bi_t = 0.01$.

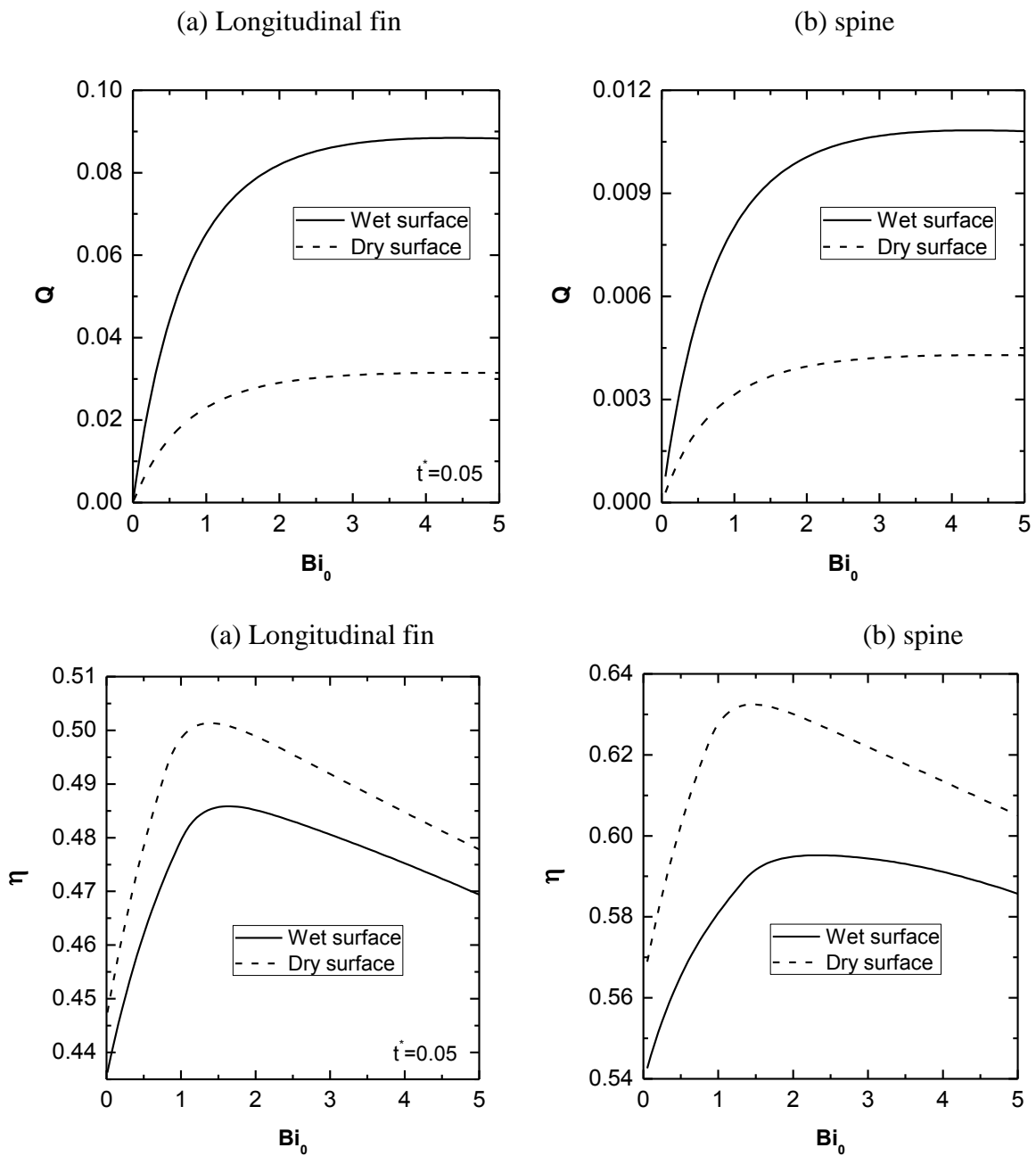


Fig. 3.9 Heat transfer and fin efficiency as a function of base Biot number.

Figs. 3.9a and 3.9b show that the base Biot number of the fin greatly influences the heat transfer rate. The fin geometry also significantly affects the heat transfer rate for both fin surface conditions. The wet surface for both the geometries gives a sudden rise in heat transfer rate with a slight increase in the Biot number. The difference in the heat transfer rate between

wet and dry fins increases significantly with Bi_0 for lower values of Bi_0 . However, this difference is maximum at a particular value of Bi_0 and beyond this, the difference does not change significantly with Bi_0 . Figs. 3.9c and 3.9d show the variation of the fin efficiency with Bi_0 . Here, in case of spine profile, a significant difference between the dry and the wet surfaces based fin efficiency is observed. Furthermore, under a given condition, there is a maximum fin efficiency at a particular Bi_0 for both dry and wet fin surface conditions. Hence, this optimum design condition can be of great importance from the practical applications.

CHAPTER-4

Heat transfer improvement of a wet fin under transient response with a unique design arrangement aspect.

4.1 Introductions

New fin designs and optimum fin shapes are the epicentres of recent research. The upcoming refrigeration and air conditioning applications require new changes in fin design, which can transfer heat efficiently under low-temperature ranges. In these applications, the base temperature is kept at a lower value than the surrounding air's dew point temperature, which strikes the fin surface, forming a thin saturated moisture layer and inducing the heat mass transfer phenomenon.

In this chapter, the author attempted the new fin design problem, which addresses the non-Fourier heat transfer on the wet surface of the longitudinal and pin fins under dehumidification.

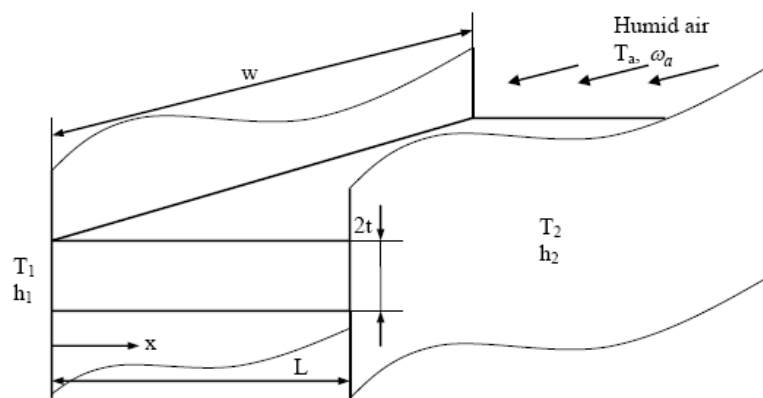
In proposed novel fin design arrangement involves dual primary fin surfaces, also called fin bases. Fourier and non-Fourier heat transfer effects are investigated with various wet fin and surface conditions design parameters. A comparative result shows how air dehumidification in fins promotes waviness in the temperature distribution curve. It is concluded from the present study that the proposed new fin design considerably enhances the heat transfer rate when compared with the conventional fin design in usage. Thus, this is a revolutionary attempt to

provide a compact fin design arrangement that provides additional mechanical strength, saving space utilization and reducing overall manufacturing costs.

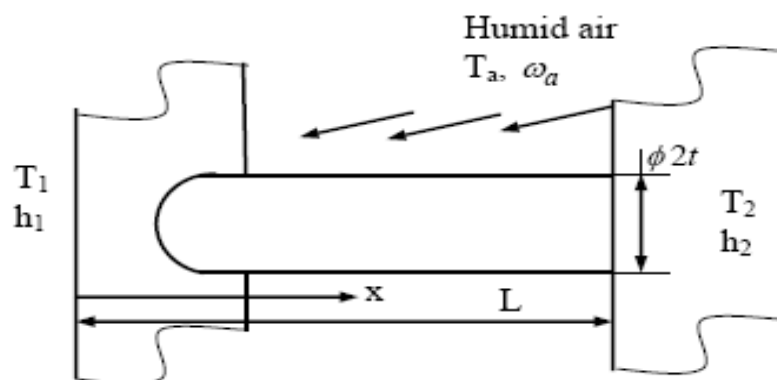
4.2 Mathematical formulations

A schematic diagram of longitudinal and pin fins with semi-thickness t , width w and length L

is shown in Fig. 4.1.



(a) Longitudinal Fin



(b) Pin Fin

Fig. 4.1 Schematic diagram of longitudinal and pin fins with asymmetric cooling on both the ends.

Two boundary conditions are used to analyze the transient effect on temperature distribution on the fin surface. With non-Fourier heat conduction [71], the governing equation for one-dimensional heat transfer with constant heat transfer coefficient under the effect of dehumidification and considering thermal relaxation time can be written as,

$$\frac{\partial^2 T}{\partial x^2} + \frac{ph}{kA_c}(T_a - T) + \frac{ph_m}{kA_c}(\omega_a - \omega)h_{fg} = \frac{\rho c_p}{k} \cdot \left(\tau_r \frac{\partial^2 T}{\partial t^2} + \frac{\partial T}{\partial t} \right) \quad (4.1)$$

In cooling applications, the fin surface is covered with saturated humid air. The humidity ratio of saturated air ω is a function of temperature according to the psychrometric relationship.

From the chart this relationship can be approximated by a linear one ($\omega = A + BT$), for a small temperature variation in the fin for the above application. Eq. (4.1) can be written in dimensionless form as,

$$\frac{\partial^2 \phi}{\partial X^2} - m^2 \phi = Ve^2 \frac{\partial^2 \phi}{\partial \tau^2} + \frac{\partial \phi}{\partial \tau} \quad (4.2)$$

where

$$\theta = \frac{T_a - T}{T_a - T_r}; \quad X = \frac{x}{L}; \quad Z_0 = L \sqrt{\frac{ph}{kA_c}}; \quad \tau = \frac{\alpha t}{L^2}; \quad \alpha = \frac{k}{\rho c_p}; \quad Ve^2 = \sqrt{\frac{\tau_r \alpha}{L^2}}$$

$$t^* = \frac{t}{w}; \quad Bi = \frac{ht}{k}; \quad \psi = \frac{t}{L}; \quad m = \sqrt{\left[(2-n)t^* + n \right] \frac{Bi}{\psi^2} (1 - B\zeta)}; \quad \phi = \theta + \theta_p;$$

$$\omega = A + BT; \quad \zeta = \frac{h_{fg}}{c_p L_e^{2/3}}; \quad \theta_p = \frac{(\omega_a - A - BT_a)\zeta}{(T_a - T_r)(1 + B\zeta)}; \quad A = \frac{\omega_r T_d - \omega_d T_r}{T_d - T_r}; \quad B = \frac{\omega_d - \omega_r}{T_d - T_r} \quad (4.3)$$

T_r and T_d reference temperature and dew point temperature, respectively. At first base (base-I), this reference temperature is equal to the fluid temperature for convection boundary condition and isothermal boundary condition.

If the Vernotte number Ve reduces to zero, Eq. (2) becomes a governing equation for Fourier heat conduction in fins as,

$$\frac{\partial^2 \phi}{\partial X^2} - m^2 \phi = \frac{\partial \phi}{\partial \tau} \quad (4.4)$$

Generally, two boundary conditions associated with the fin tip and fin base are considered for one-dimensional heat conduction analysis. The base temperature is assumed to be constant, and the tip is insulated to simplify the analysis in conventional cases with a fin single base surface. For such fin arrangements, heat transfer from the fin surface at the fin tip reduces, and it can be observed that the material of constant thickness fins does not effectively participate in transferring heat. Alternatively, varying fin thickness can overcome this difficulty, but these fins are challenging to manufacture and fabricate. Because of this practical difficulty, the author of the present study has suggested a novel fin design having two base surfaces to improve the heat transfer rate. In this design, unlike conventional fins, the fin tip is also attached to primary surfaces at both ends. These primary surfaces are separately considered for two boundary conditions, viz., convective base and isothermal base. It is important to note here that, in the present study, the fin tip does not exist as it is attached to two bases, called

primary surfaces of the fins. For the solution of Eq. (4.2), possible practical initial and boundary conditions (Fig. 4.1) are written mathematically as,

$$\text{at } \tau = 0 \quad (0 \leq X \leq 1), \quad \phi(X, \tau) = \theta_0 \quad (4.5a)$$

$$\text{at } \tau = 0 \quad (0 \leq X \leq 1), \quad \frac{\partial \phi(X, \tau)}{\partial \tau} = 0 \quad (4.5b)$$

and

$$\begin{cases} \text{at } X = 0 \quad (\tau > 0), & \phi(X, \tau) = \theta_0 \\ \text{at } X = 1 \quad (\tau > 0), & \phi(X, \tau) = \theta_L \end{cases} \quad \text{(Constant base temperature)} \quad (4.5c)$$

$$\begin{cases} \text{at } X = 0 \quad (\tau > 0), & \frac{\partial \phi}{\partial X} = Bi_1(\phi - \phi_0) \\ \text{at } X = 1 \quad (\tau > 0), & \frac{\partial \phi}{\partial X} = -Bi_2(\phi - \phi_L) \end{cases} \quad \text{(Convected base condition)} \quad (4.5d)$$

where

$$\phi_0 = 1 + \theta_p ; \phi_L = \theta_L + \theta_p ; \theta_L = \frac{T_a - T_2}{T_a - T_r} \quad (4.5e)$$

Where $Bi_1 = h_1L/k$ and $Bi_2 = h_2L/k$. These two Biot numbers represent the heat transfer from the primary surfaces at both ends of the fin to the surrounding. The boundary conditions for the solution of Fourier heat conduction in the fin (Eq.(3)) can be taken the same as expressed in Eqs. (4a), either (4c) or (4d) for comparison between Fourier and non-Fourier analysis. The governing equation (Eq.(2)) and the boundary conditions (Eq.(4)) are non-homogeneous. To obtain an analytical solution, separation of variables can be employed for Eq.(2) for non-Fourier heat conduction and may be initially required to convert homogeneous equations using new variables as

$$\phi(X, \tau) = \Gamma(X) + \Omega(X, \tau) \quad (4.6)$$

Eq. (4.2) can be written by using Eq. (4.6) by separating the dependent variables as

$$\frac{d^2\Gamma}{dX^2} - m^2\Gamma = 0 \quad (4.7a)$$

and

$$\frac{\partial^2\Omega}{\partial X^2} - m^2\Omega = Ve^2 \frac{\partial^2\Omega}{\partial \tau^2} + \frac{\partial\Omega}{\partial \tau} \quad (4.7b)$$

For the solution of equation (4.7), the initial and boundary conditions are obtained by combining Eq. (4.5) and (4.6) as,

$$at \quad \tau = 0 \quad (0 \leq X \leq 1), \quad \Gamma(X) + \Omega(X, \tau) = \theta_p \quad (4.8a)$$

$$at \quad \tau = 0 \quad (0 \leq X \leq 1), \quad \frac{\partial\Omega(X, \tau)}{\partial \tau} = 0 \quad (4.8b)$$

$$X = 0 \quad (\tau > 0),$$

$$\begin{cases} \Gamma(X) = \phi_0 \\ \Omega(X, \tau) = 0 \end{cases} \quad (\text{Constant base temperature}) \quad (4.8c)$$

$$at \quad X = 0 \quad (\tau > 0),$$

$$\begin{cases} \frac{\partial\Gamma(X)}{\partial X} - Bi_1[\Gamma(X) - \phi_0] = 0 \\ \frac{\partial\Omega(X, \tau)}{\partial X} - Bi_1\Omega(X, \tau) = 0 \end{cases} \quad (\text{Convected base condition}) \quad (4.8d)$$

$$at \quad X = 1 \quad (\tau > 0),$$

$$\begin{cases} \Gamma(X) = \phi_L \\ \Omega(X, \tau) = 0 \end{cases} \quad (\text{Constant base temperature}) \quad (4.8e)$$

$$at \quad X = 1 \quad (\tau > 0),$$

$$\begin{cases} \frac{\partial\Gamma(X)}{\partial X} + Bi_2[\Gamma(X) - \phi_L] = 0 \\ \frac{\partial\Omega(X, \tau)}{\partial X} + Bi_2\Omega(X, \tau) = 0 \end{cases} \quad (\text{Convected base condition}) \quad (4.8f)$$

The solution of Eq. (4.7a) is divided into two parts for the isothermal base and the convected base, which can be obtained from boundary conditions (4.8c), (4.8e), and (4.8d), (4.8f), respectively as,

$$\Gamma(X) = \frac{\phi_1 \sinh[m(1-X)] + \phi_L \sinh(mx)}{\sinh m} \quad (4.9a)$$

and

$$\Gamma(X) = A_1 \cosh[m(1-X)] + A_2 \sinh[m(1-X)] + A_3 \cosh(mX) + A_4 \sinh(mX) \quad (4.9b)$$

where

$$A_1 = \frac{\phi_0 m Bi_1}{(m^2 + Bi_1 Bi_2) \sinh m + m(Bi_1 + Bi_2) \cosh m} \quad (4.10a)$$

$$A_2 = \frac{Bi_1 Bi_2 \phi_0}{(m^2 + Bi_1 Bi_2) \sinh m + m(Bi_1 + Bi_2) \cosh m} \quad (4.10b)$$

$$A_3 = \frac{\phi_L Bi_2 m}{(m^2 + Bi_1 Bi_2) \sinh m + m(Bi_1 + Bi_2) \cosh m} \quad (4.10c)$$

$$A_4 = \frac{Bi_1 \phi_L Bi_2}{(m^2 + Bi_1 Bi_2) \sinh m + m(Bi_1 + Bi_2) \cosh m} \quad (4.10d)$$

In order to determine $\Omega(X, \tau)$ Eq. (4.7b) can be solved by the product method. For this method, it is assumed that $\Omega(X, \tau) = E(X) \cdot F(\tau)$ for constant temperature base and $\Omega(X, \tau) = U(X) V(\tau)$ for convected base conditions respectively. Using this relationship,

Eq.(4.7b) and (4.8) can be expressed by separating the two variables as:

$$\frac{d^2 E}{dX^2} + \lambda^2 E = 0 \quad \text{and} \quad \frac{d^2 U}{dX^2} + \lambda^2 U = 0 \quad (4.11a)$$

$$Ve^2 \frac{d^2 F}{d\tau^2} + \frac{dF}{d\tau} + F(m^2 + \lambda^2) = 0 \quad \text{and} \quad Ve^2 \frac{d^2 V}{d\tau^2} + \frac{dV}{d\tau} + V(m^2 + \lambda^2) = 0 \quad (4.11b)$$

$$E(X)F(0) + \Gamma(X) = \phi_p \quad \text{and} \quad U(X)V(0) + \Gamma(X) = \phi_p \quad (4.12a)$$

$$\frac{dF(0)}{d\tau} = 0 \quad \text{and} \quad \frac{dV(0)}{d\tau} = 0 \quad (4.12b)$$

$$E(0) = 0 \quad \text{and} \quad E(1) = 0 \quad (\text{Constant base temperature}) \quad (4.12c)$$

$$\frac{dU(0)}{dX} - Bi_1 U(0) = 0 \quad \text{and} \quad \frac{dU(1)}{dX} + Bi_2 U(1) = 0 \quad (\text{Convected base condition}) \quad (4.12d)$$

From Eqs. (4.11a) and (4.12c)) one can obtain the following relationship:

$$\lambda_i = i\pi \quad \text{for} \quad 0, 1, 2, 3, \dots \quad (4.13a)$$

Combining Eqs. (4.11a) and (4.12d) yields,

$$\lambda_j = j\pi - \tan^{-1} \frac{\lambda_j (Bi_1 + Bi_2)}{Bi_1 Bi_2 - \lambda_j^2} \quad \text{for} \quad 0, 1, 2, 3, \dots \quad (4.13b)$$

Eigen values, λ_i and λ_j are determined from Eqs. (4.13a) and (4.13b), respectively. In order

to determine λ_j , Newton-Raphson iterative method is used to solve the transcendental Eq.

(4.13b) for each value of j. The final iterative value of λ_j has been evaluated by satisfying

the necessary and sufficient convergence criteria. The necessary convergence criterion is taken

as 10^{-6} . From Eqs. (4.6) - (4.11), $\phi(X, \tau)$ can then be derived for isothermal and convected

bases respectively as,

$$\phi(X, \tau) = \frac{\phi_0 \sinh[m(1-X)] + \phi_L \sinh(mx)}{\sinh m} + \left\{ \begin{array}{l} \sum_{i=0}^{\infty} \frac{2 \sin(\lambda_i X) G_i}{D_{1i} - D_{2i}} [D_{1i} e^{D_{2i}} - D_{2i} e^{D_{1i}}] \quad \text{for} \quad 1 - V_e^2 (\lambda_i^2 + m^2) > 0 \\ \sum_{i=0}^{\infty} G_i 2 \sin(\lambda_i X) (1 - D_0 \tau) e^{D_0 \tau} \quad \text{for} \quad 1 - V_e^2 (\lambda_i^2 + m^2) = 0 \\ \sum_{i=0}^{\infty} \frac{2 G_i}{E_i} [E_i \cos(E_i \tau) - D_0 \sin(E_i \tau)] e^{D_0 \tau} \sin(\lambda_i X) \quad \text{for} \quad 1 - V_e^2 (\lambda_n^2 + m^2) > 0 \end{array} \right.$$

$$(4.14a)$$

and

$$\begin{aligned} \phi(X, \tau) = & A_1 \cosh[m(1-X)] + A_2 \sinh[m(1-X)] + A_3 \cosh(mX) + A_4 \sinh(mX) \\ & + \begin{cases} \sum_{j=0}^{\infty} C_j \cos(\beta_j - \lambda_j X) e^{D_0 \tau} \left[(D_0 + E_j) e^{-E_j \tau} - (D_0 - E_j) e^{E_j \tau} \right] & \text{for } 1 - 4V_e^2 (Z_0^2 + \lambda_j^2) > 0 \\ \sum_{j=0}^{\infty} C_j \cos(\beta_j - \lambda_j X) (1 - D_0 \tau) e^{D_0 \tau} & \text{for } 1 - 4V_e^2 (Z_0^2 + \lambda_j^2) = 0 \\ \sum_{j=0}^{\infty} C_j \cos(\beta_j - \lambda_j X) e^{D_0 \tau} \left[E_j \cos(E_j \tau) - D_0 \sin(E_j \tau) \right] & \text{for } 1 - 4V_e^2 (Z_0^2 + \lambda_j^2) < 0 \end{cases} \end{aligned} \quad (4.14b)$$

$$(D_{1i}, D_{2i}, D_{1j}, D_{2j}) = \left(\frac{-1 \pm \sqrt{1 - 4V_e^2 (m^2 + \lambda_i^2)}}{2V_e^2}; \frac{-1 \pm \sqrt{1 - 4V_e^2 (m^2 + \lambda_j^2)}}{2V_e^2} \right) \quad (4.15a)$$

$$(E_i, E_j) = \frac{\sqrt{4V_e^2 (m^2 + \lambda_i^2) - 1}}{2V_e^2}; \frac{\sqrt{4V_e^2 (m^2 + \lambda_j^2) - 1}}{2V_e^2} \quad (4.15b)$$

$$G_i = \frac{\theta_p}{\lambda_i} (1 - \cos \lambda_i) - \frac{\lambda_i}{(\lambda_i^2 - m^2)} (\phi_0 - \phi_L \cos \lambda_i) \quad (4.15c)$$

and

$$(D_0; \beta_j) = \left(\frac{-1}{2V_e^2}; \tan^{-1} \frac{Bi_1}{\lambda_j} \right) \quad (4.15d)$$

From the orthogonal condition, the constant 'C_j' is determined from the initial condition

expressed in eq. (4.12a) and can be written explicitly for convected base condition as follows:

$$C_j = \begin{cases} \frac{2\lambda_i}{E_j} I_{1j}^{-1} I_{2j}; & 1 - 4V_e^2 (Z_0^2 + \lambda_j^2) > 0 \\ 4\lambda_j I_{1j}^{-1} I_{2j}; & 1 - 4V_e^2 (Z_0^2 + \lambda_j^2) = 0 \\ 4\lambda_j I_{1j}^{-1} I_{2j}; & 1 - 4V_e^2 (Z_0^2 + \lambda_j^2) < 0 \end{cases} \quad (4.16a)$$

where

$$I_{1j} = [2\lambda_j + \sin(2\beta_j) - \sin\{2(\beta_j - \lambda_j)\}] \quad (4.16b)$$

and

$$I_{2j} = \left[\begin{aligned} & \frac{\phi_p}{\lambda_j} \{ \sin \beta_j - \sin(\beta_j - \lambda_j) \} \\ & - \frac{A_1}{(m^2 + \lambda_j^2)} \{ \lambda_j \cosh(m) \sin(\beta_j) - \lambda_j \sin(\beta_j - \lambda_j) + m \sinh(m) \cos(\beta_j) \} \\ & - \frac{A_2}{(m^2 + \lambda_j^2)} \{ \lambda_j \sinh(m) \sin(\beta_j) - m \cos(\beta_j - \lambda_j) + m \cosh(m) \cos(\beta_j) \} \\ & - \frac{A_3}{(m^2 + \lambda_j^2)} \{ \lambda_j \sin \beta_j - \lambda_j \cosh(m) \sin(\beta_j - \lambda_j) + m \sinh(m) \cos(\beta_j - \lambda_j) \} \\ & - \frac{A_4}{(m^2 + \lambda_j^2)} \{ m \cosh(m) \cos(\beta_j - \lambda_j) - m \cos(\beta_j) - \lambda_j \sinh(m) \sin(\beta_j - \lambda_j) \} \end{aligned} \right] \quad (4.16c)$$

In the case of Fourier heat transfer, the following temperature distribution can be derived from

Eqs. (4.4), (4.5a), and (4.5c) for the isothermal base and from Eqs. (4.4), (4.5a), and (4.5d)

for the convected base, and they can be written, respectively as,

$$\begin{aligned} \phi(X, \tau) = & \frac{\phi_0 \sinh[m(1-X)] + \phi_L \sinh(mx)}{\sinh m} \\ & + 2 \sum_{i=1}^{\infty} e^{-(\lambda_i^2 + m^2)\tau} \sin(\lambda_i X) \left[\frac{\phi_p}{\lambda_i} (1 - \cos \lambda_i) - \frac{\lambda_i}{(\lambda_i^2 + m^2)} (\phi_0 - \phi_L \cos \lambda_i) \right] \end{aligned} \quad (4.17a)$$

and

$$\begin{aligned} \phi(X, \tau) = & A_1 \cosh[m(1-X)] + A_2 \sinh[m(1-X)] + A_3 \cosh(mX) + A_4 \sinh(mX) \\ & + \sum_{j=0}^{\infty} 4\lambda_j I_{1j}^{-1} \cdot I_{2j} e^{-(m^2 + \lambda_j^2)\tau} \cos(\beta_j - \lambda_j X) \end{aligned} \quad (4.17b)$$

The average temperature in the fin is determined from Eq. (4.17) by integration as,

$$\phi_{av}(\tau) = \int_{X=0}^1 \phi(X, \tau) dX \quad (\tau > 0) \quad (4.18a)$$

The ideal heat transfer rate in wet in can be determined using the instantaneous minimum fin surface temperature, and it is evaluated from the temperature expression written in Eq. (4.14)

by varying the spatial coordinate X. However, it is noted that, in the case of the Fourier heat transfer, the minimum wet fin temperature is always the base temperature. This chapter considers two base surfaces with different temperatures, from which the base maintaining a lower temperature must be taken. The instantaneous actual heat transfer rate (q) and ideal heat transfer rate (q_i) can be evaluated based on the integral approach written in dimensionless form as,

$$\begin{cases} Q(\tau) = \frac{q(\tau) + Bi_L \phi_L}{hpL(T_a - T_r)} = (1 + B\zeta) \int_{X=0}^1 \phi(X, \tau) dX, \\ Q_i(\tau) = \frac{q_i(\tau) + Bi_L \phi_L}{hpL(T_a - T_r)} = (1 + B\zeta) \phi(X_m, \tau) \end{cases} \quad (4.18b)$$

where, X_m is the location having a minimum dimensional temperature. From the definition, the instantaneous efficiency can be, by using Eqs. (4.18a) and (4.18b) and the following expression can be obtained;

$$\eta(\tau) = \frac{\phi_{av}(\tau)}{\phi(X_m, \tau)} \quad (4.19)$$

where $\phi(X_m, \tau)$ is the maximum dimensional temperature parameter. The fin effectiveness

can be determined from the following expression;

$$\varepsilon(\tau) = \frac{[n + (2-n)t^*] \phi_{av}}{\psi(\phi_0 + \phi_L)} \quad (4.20)$$

Where ϕ_0 and ϕ_L are the temperature parameter at the base of the fin from which x- coordinate starts and ends, respectively. Here it can be noted for finding ϕ_0 and ϕ_L under convective base

boundary conditions, the temperature distribution for non-Fourier and Fourier heat transfer (Eqs. (4.14) and (4.17)) is used.

4.3 Results and discussion

Unlike much research done by earlier researchers on conventional fin design, the work presented here proposes a new fin design criterion and fin arrangement to study the fin response under the effect of dehumidification. The two boundary conditions are applied to investigate this effect under Fourier and non-Fourier laws. Some dimensionless parameters like Fourier number, Vernotte number, and Biot number at the two primary base surfaces are selected for the analysis. A closed-form classical technique called separation of variables determines instantaneous fin performance under Fourier and non-Fourier laws.

4.4 Validation of the present research work

Before presenting the results of the present study, it is always necessary to validate the mathematical analysis with that of the earlier research work carried out by researchers. Fig. 2 shows the comparison of the temperature distribution in fins obtained from the present work and the published work (Kundu and Lee, 2013).

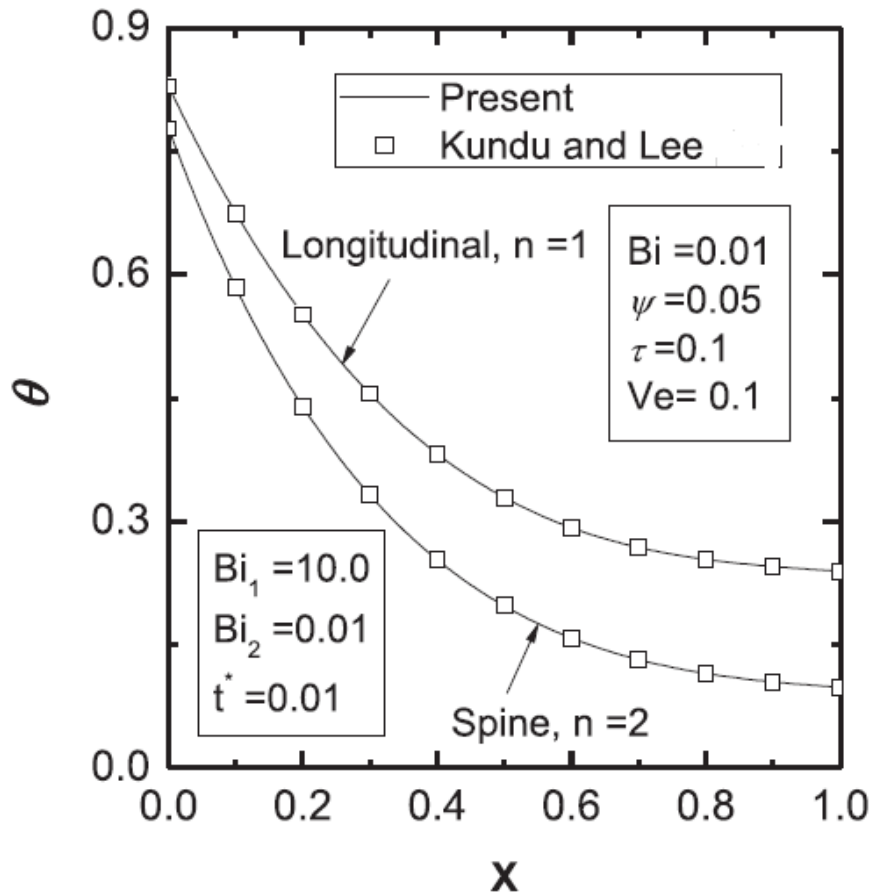


Fig. 4.2 Comparison of temperature distribution in fins obtained from the present work and the published work for consideration of the dry surface having a single base.

In the above figure and its analysis, non-Fourier heat transfer with dry fin surface condition and a single fin base is considered. Hence to obtain the local fin temperature profile, one of the bases in the present analysis is also maintained at the convective condition with a Biot number, $Bi_1 = 10$, however, the analysis for another end of the fin is made at a very low Biot number, $Bi_2 = 0.01$. As dry fin surface condition is considered, the value of dehumidification parameter, ζ in the present study is taken zero. Low values of Vernotte number and Fourier number in the transient heat transfer on a dry surface show the above work's temperature distribution pattern precisely matches the previous study reported by Kundu and Lee. Fig. 3

compares the temperature distribution in wet fins predicted by the present analysis and numerical methods. The numerical solution is obtained using the finite difference method, which involves central differencing for space discretization, and an implicit scheme for the time is adopted. The analysis covers the set of various thermo-physical parameters, as depicted in Fig. 3.

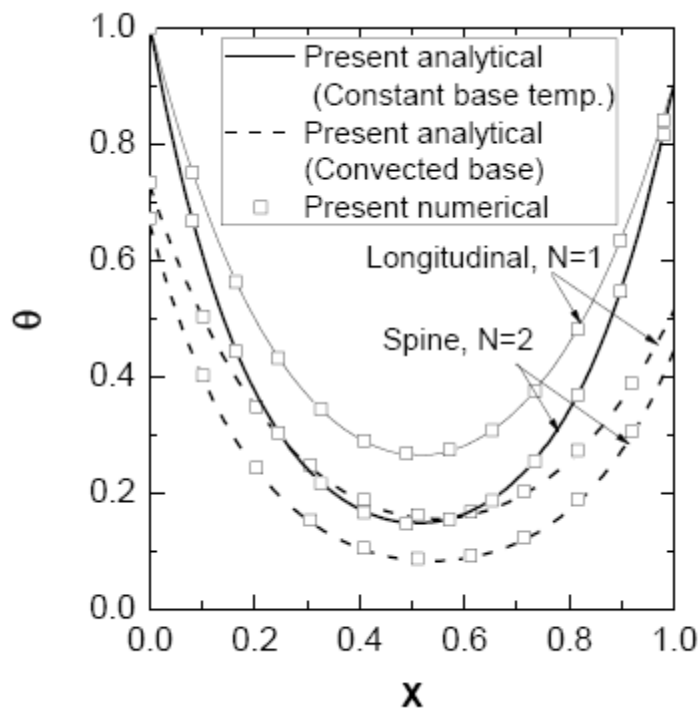


Fig. 4.3 Comparison of the temperature distribution in wet fins predicted by the present analysis and numerical methods.

As shown in Fig. 1, the fin tips are attached to the primary surfaces on both sides. The temperature distribution of the fin surface is studied by maintaining the temperature at both the primary surfaces at different temperatures, as indicated before. The temperature difference between two primary surfaces is maintained low to avoid the formation of thermal stresses and their effect on fin geometry. Comparing the second base surface, a higher value of Biot number

at the first base surface shows the convection at a high rate. As predicted, the temperature distribution pattern for longitudinal and pin fins under constant temperature and convective base conditions shows a similar trend. A lower temperature value near the middle part of the curve is observed, similar to that of the fin tip behavior of a conventional fin when the base is at either constant temperature or at a convective condition with the fin tip insulated. The minimum temperature precisely at the middle portion occurs at both ends of a fin are maintained with similar boundary conditions. Therefore, it can be well inferred that the present system of fin design results in better fin performance. The numerical solution verifies the analytical results, and both are found well in line.

4.5 A novel fin design approach for heat transfer improvement

In the present chapter, a systematic study has been carried out to identify the effect of dehumidification of air on the fin surface in refrigeration and air conditioning applications. For generating the results, some design values have been taken as constant. These values are $Bi_1 = 0.01$, $\psi = 0.05$, $t^* = 0.01$, $p_a = 1.013$ bars, $T_1 = 1^\circ C$, $T_2 = 4^\circ C$, $T_a = 32^\circ C$, and $RH = 100$ % . It can be noted here; these design values have been selected arbitrarily to get result trends from present analysis. The remaining values can be taken in order to obtain unknown parameters depending upon the design requirement.

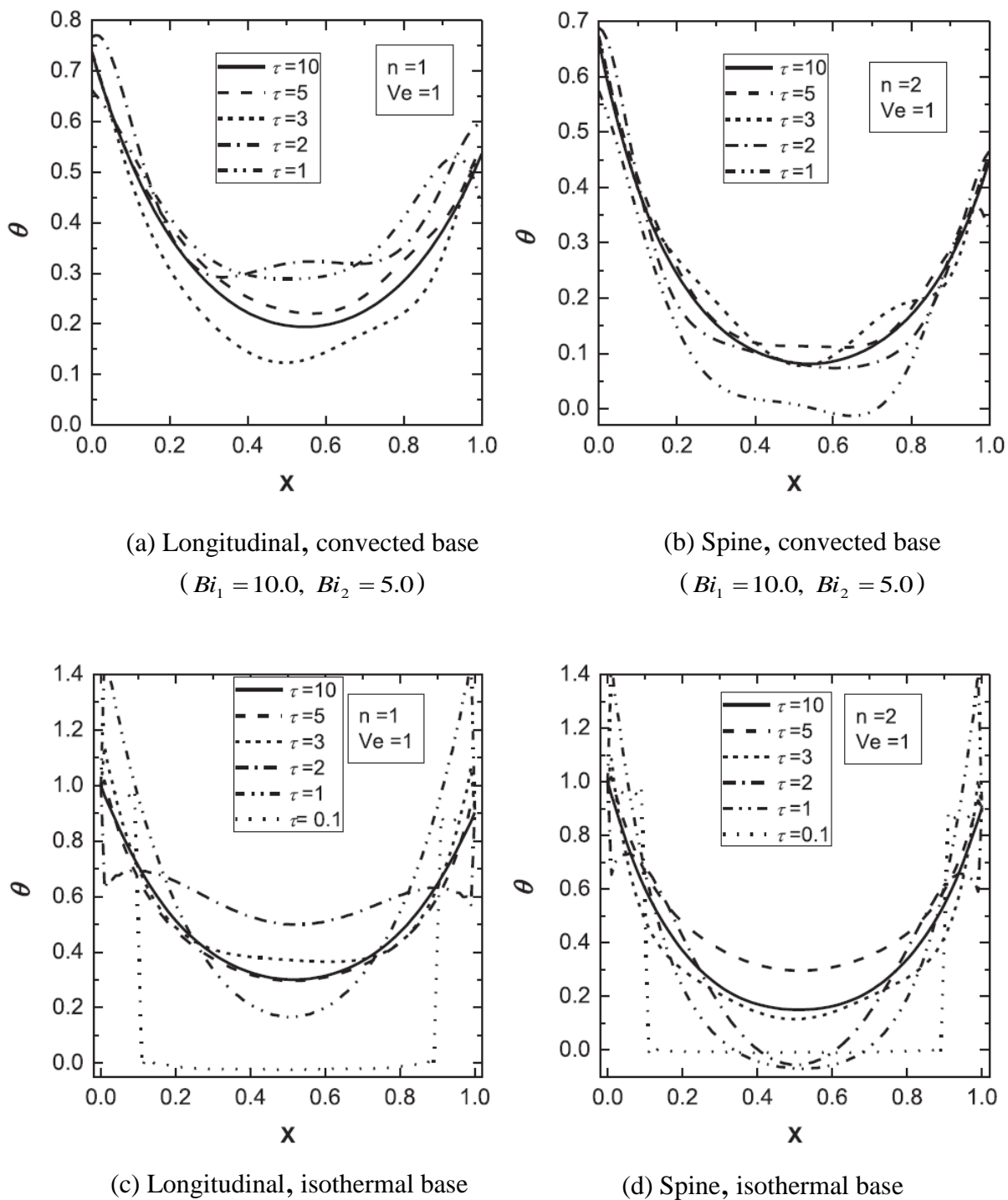


Fig. 4.4 Non- Fourier temperature distribution in wet fins as a function of dimensionless time, τ .

Fig. 4.4 depicts the non-Fourier local temperature distribution in wet fins as a function of dimensionless time at different values of the Fourier number, τ . Different fin geometries (i.e., longitudinal and spine) have been considered with convected base (Fig. 4.4a and b) and

isothermal (Fig. 4.4 c and d) base conditions for presenting the results. Figs. 4 (a) and (b) show that, as the Fourier number, τ increases, the spatial temperature in the fin approaches the respective base temperatures to reach a steady temperature. However, at lower values of Fourier number, the curve exhibits a peculiar nature for dominating non-Fourier nature towards the middle part of the curve, indicating a slower heat conduction rate and faster surface heat transfer. Both fin geometries show similarities in their curve behavior. Fig. 4 (c) and (d) illustrate the isothermal base condition for longitudinal and pin fins, respectively. The primary surfaces of the fins are maintained at different temperatures while analyzing the non-Fourier heat conduction behavior in fins. It can be seen that at lower values of the Fourier number and at a specific Vernotte number, the heat wave observes more amplitude and takes considerable time to become steady. At constant base temperature, an irregular variation is observed in non-Fourier temperature distribution in the fin as a function of τ . It is crucial to note that, though the fin is maintained at temperatures at both the primary surfaces, the middle part of the fin behaves like the conventional fin tip, which is self-explanatory to prove the correctness of the solution presented here. The non-Fourier heat conduction equation for the fin is hyperbolic; hence, the transient temperature response may not always have a consistent trend to reach a stable state from an unstable condition. However, this stable state condition does not depend on the method of heat conduction in fins, whether Fourier or non-Fourier approach.

Fig. 4.5 shows the Fourier and non-Fourier temperature response in fins as a function of different design conditions. The dry and wet fin surfaces under the fin base's isothermal and convective conditions are considered to record the transient thermal response.

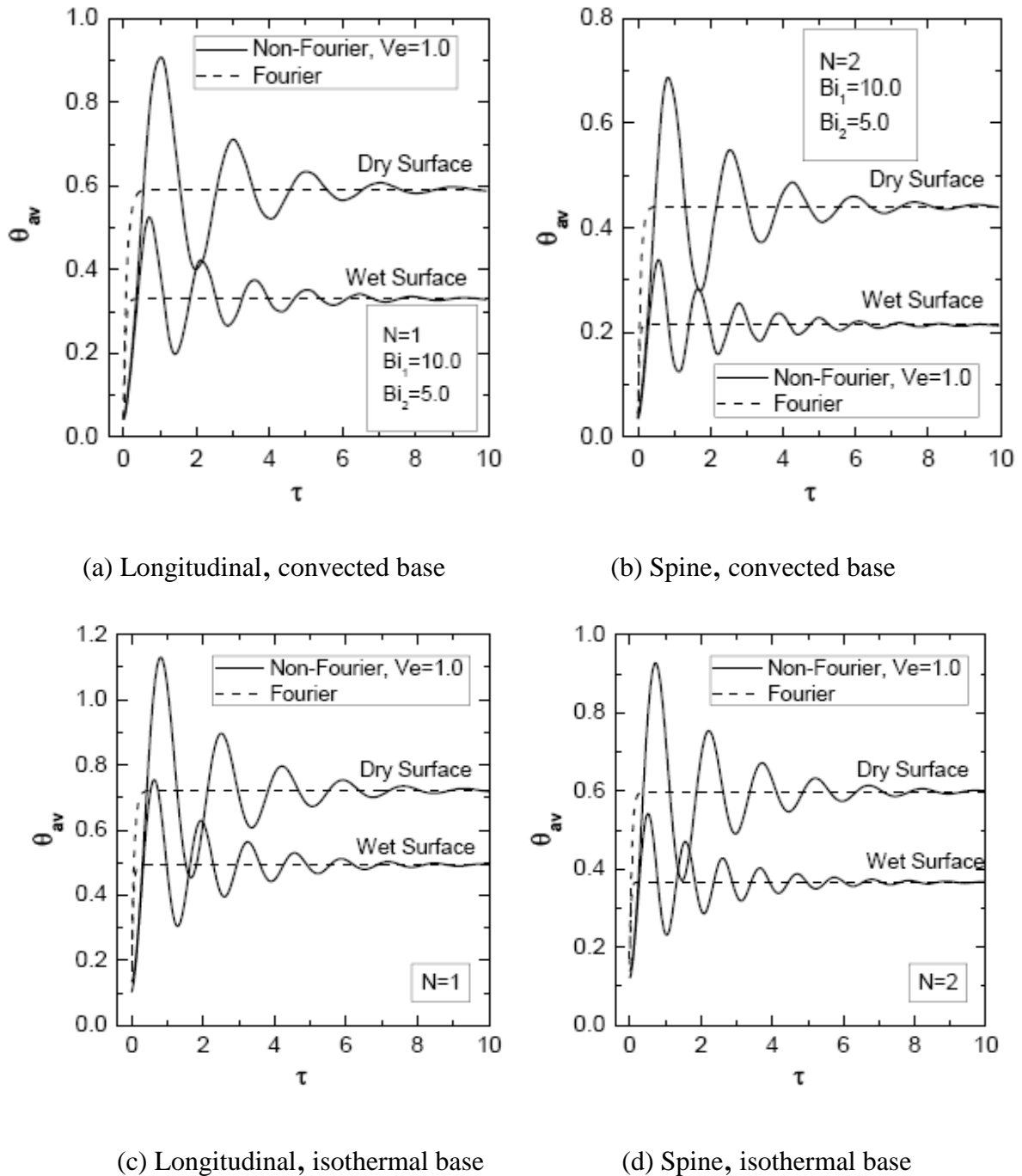
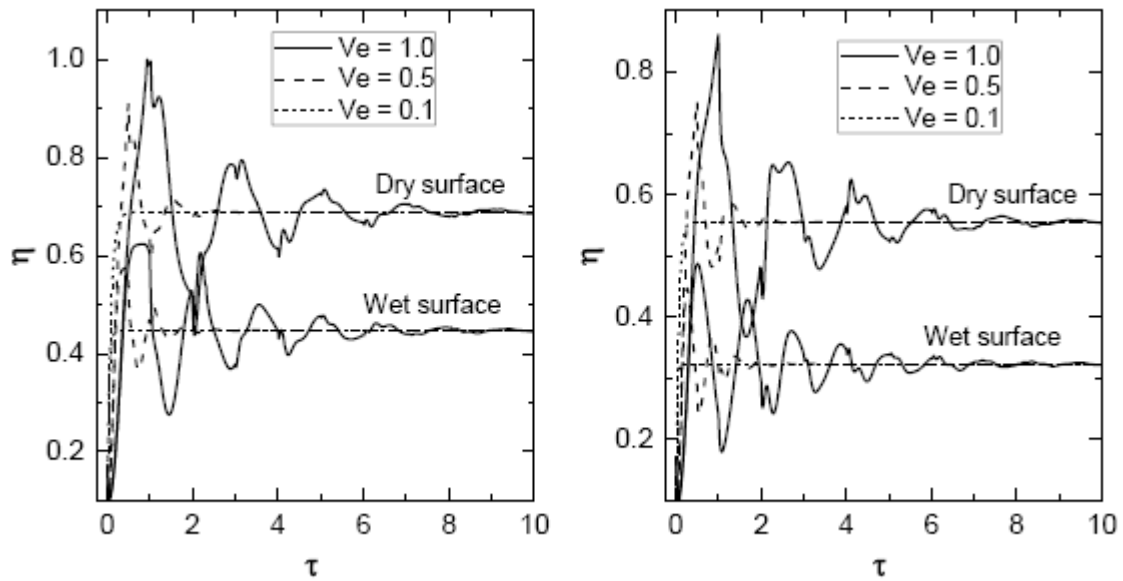


Fig. 4.5 Fourier and non-Fourier temperature response in fins as a function of different design conditions.

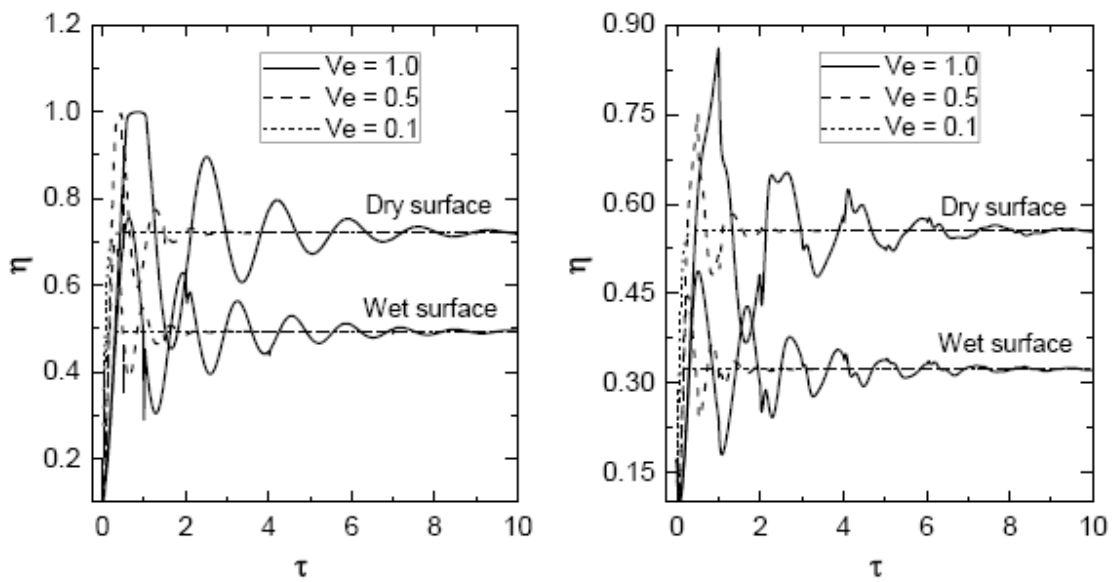
As can be observed in Fig. 4.5, the difference in the temperature response between Fourier and non-Fourier models is remarkable at lower values of Fourier number, τ due to finite speed of heat wave propagation for non-Fourier model. This difference gradually diminishes with higher values of τ and the speed of the thermal wave in non-Fourier model approaches to that of Fourier one. However, at lower values of τ , the non-Fourier temperature response looks sinusoidal in nature for hyperbolic governing equation. The mean line of the heat curve may be representing the Fourier temperature response. It can also be observed that the dehumidification effect in the case of wet fin surface enhances the waviness and increases the amplitudes in the thermal wave when compared with dry fin surface. It can be concluded here that; a wet fin surface is more sensitive to non-Fourier heat conduction than a dry surface. It has been noticed again that the convective fin base condition gives a smoother temperature response than the isothermal fin base condition because of the less restricted movement of the heat wave.

The effect of boundary conditions under dehumidification, Fourier number, and Vernotte number has also been examined for temperature distribution in the fin. The non-Fourier heat transfer dominates with the condensation due to the resistance provided by the thin layer of condensate formed on the fin surface.



(a) Longitudinal, convected base

(b) Spine, convected base



(c) Longitudinal, isothermal base

(d) Spine, isothermal base

Fig. 4.6 Fin efficiency for non-Fourier heat transfer.

Fig.4.6 shows the influence of Vernotte number on fin efficiency for both the base and fin surface conditions. Various values of Vernotte number V_e are considered to model the non-Fourier heat conduction. At higher values of Vernotte number, V_e and lower values of Fourier

number, τ the fin efficiency found to be increased probably because, initially, the fin surface temperature and the fin base temperature are almost equal to the time lag in heat wave propagation. It has also indicated that the dry fin surface provides greater fin efficiency as it has less thermal resistance than the wet fin surface involving the thin layer of condensate on its surface. Moreover, it is also observed that the fin efficiency of the longitudinal fin is slightly greater than pin fin because of its less temperature variation from base to tip.

As stated in the literature review, the main objective of this work is to determine the fin efficiency and performance in a proposed novel fin design arrangement. From Fig. 4.7 below, it can be asserted that the pin fin is more effective than the longitudinal fin for both base conditions. The difference in temperature between the fin surface and fin base in non-Fourier heat transfer is significantly less during the initial period. The pin fin has more surface area exposed to the surrounding; the fin base behaves as a unique system without a fin and dissipates heat to the surrounding.

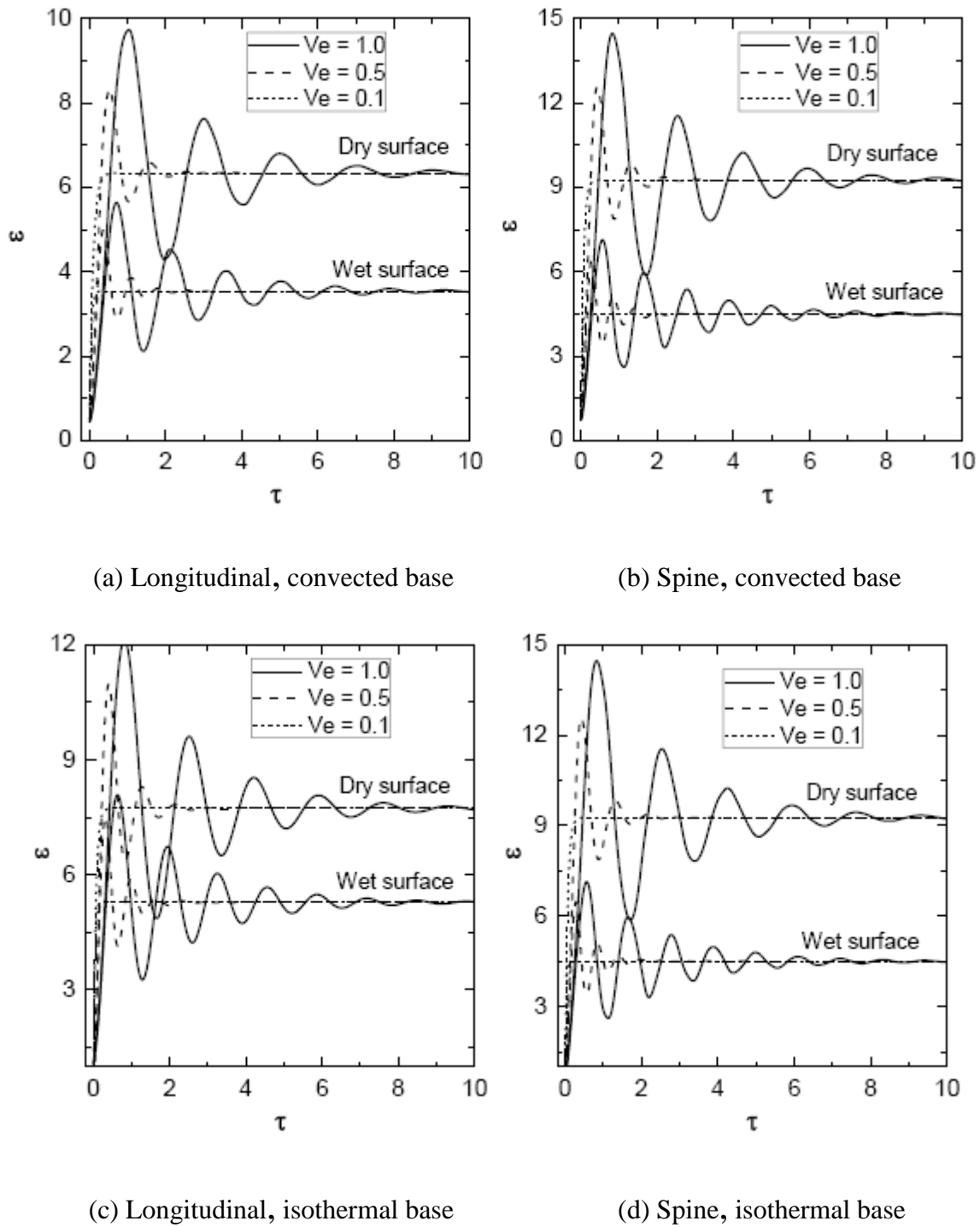


Fig. 4.7 Fin effectiveness for non-Fourier heat transfer.

It has always been a good practice in research that every proposed research has to undergo a series of tests, comparisons, and validation to prove its novelty. In this work, an exercise has been devoted to understanding the merits of the proposed work with earlier conventional work

by other researchers. Usually, a conventional fin has a single base attached to the primary surface, and the fin tip is exposed to the surrounding fluid. The fin tip is assumed to be insulated to simplify the analysis in conventional problems. In this study, the fin tip is attached to another base called a primary surface with convection or isothermal condition. Fig. 4.8 compares temperature distribution in wet fins between present and conventional cases at $V_e = 0.5$ and $\tau = 1.0$. The temperature distribution in conventional fins gradually decreases from the fin base to the fin tip, as shown in Fig. 4.8. therefore, the traditional fin has less ability to enhance the heat transfer near the tip area zone, as can be observed from this figure.

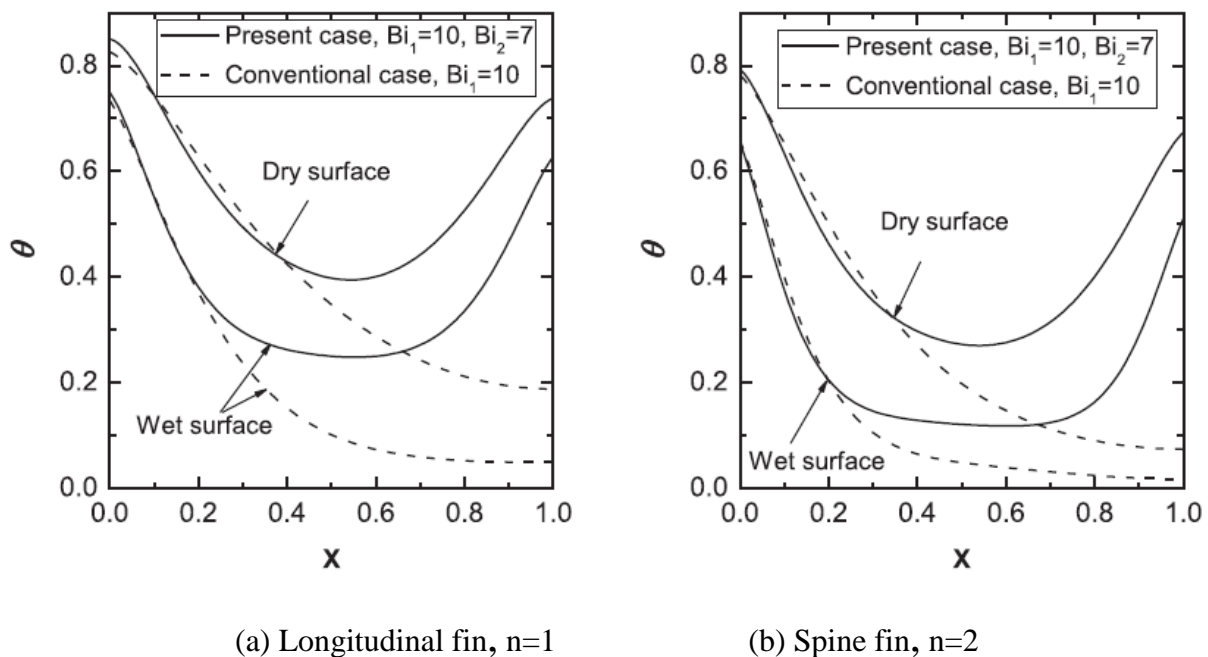


Fig. 4.8 Comparison of temperature distribution in wet fins between present and conventional cases at $V_e = 0.5$ and $\tau = 1.0$.

This negative aspect can be minimized by considering the present fin design arrangement to have an increased potential for heat transfer from both the fin ends lateral surfaces. In the current model's case, the fin's temperature distribution gradually decreases until it reaches a

minimum value, and then the temperature increases. Figs. 8a and 8b are drawn for longitudinal and pin fins, respectively. A spine's dimensionless surface temperature is slightly smaller than that of longitudinal fins. This implies that the dimensionless temperature in the case of the wet fin is marginally higher than the longitudinal fin with an identical design parameter.

Fig. 4.9 has been plotted for the average temperature of the wet longitudinal fin and pin fin as a function of dimensionless time. The results are taken by adopting the non-Fourier heat transfer analysis. A comparison of the average temperature for the conventional and the proposed fin design arrangement has been illustrated in this figure.

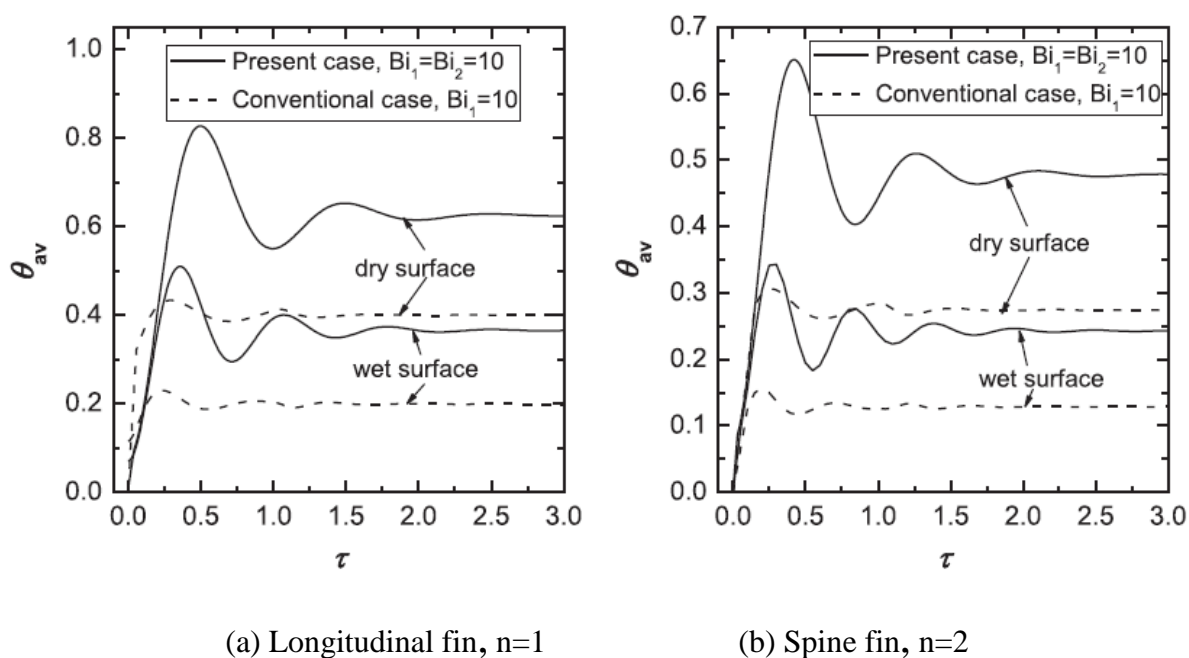


Fig. 4.9 Comparison of average temperature of dry and wet fins as a function of Fourier number between present and conventional cases for $V_e = 0.5$.

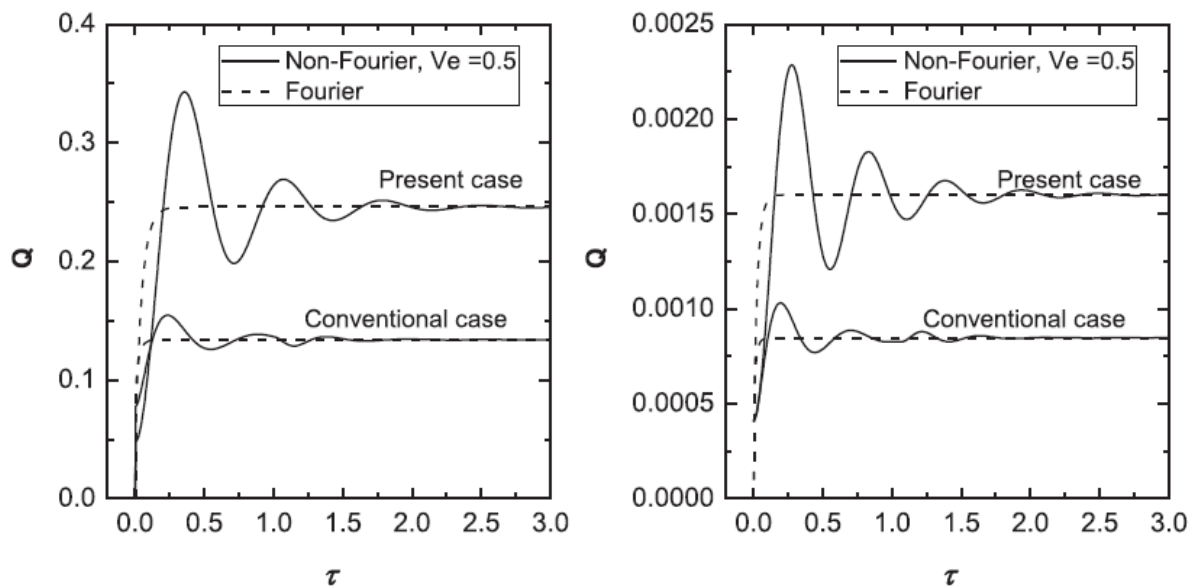
The study also covers the dry fin surface. The dimensionless average temperature of the proposed design fin is always higher than the conventional fin. However, it can be noted that at a high dimensionless temperature θ_{av} , the dimensional temperature is low. This leads to

maintaining a higher value of temperature difference between the surrounding air and fin surface for wet fins. The design aspect in the present study may have justified the advantage of the current fin design based on the enhancement of the heat transfer rate.

The main aim of the present study is to enhance the heat transfer rate through a fin with the current analysis compared to conventional fin design. For this study, Fig. 4.10 is plotted for Fourier and non-Fourier dimensionless heat transfer rate, Q as a function of Fourier number is predicted. The mathematical expression of Q for both longitudinal and pin fins has been written in dimensionless form as,

$$Q = \frac{Bi^n}{\psi} (1 + B\zeta) [1 + 2(2 - n)t^*] \phi_{av} \quad (4.21)$$

From Fig. 4.10, it can be envisaged that the heat transfer rate is strongly dependent upon the Fourier number τ towards its lower value for both Fourier and non-Fourier heat transfer. However, a strong dependency has been obtained for the non-Fourier heat transfer within a time span. On the other hand, at steady state, there is no difference in heat transfer between Fourier and non-Fourier models. A considerable difference in heat transfer rate between the present study and the conventional case has been obtained at high value of τ which indicates a superiority of the present model as well from the heat transfer rate point of view.



(a) Longitudinal fin, $n=1$

(b) Spine fin, $n=2$

Fig. 4.10 Comparison of heat transfer rate in wet fins as a function of Fourier number between present and conventional cases for $V_e = 0.5$.

The present analytical work studies temperature distribution, fin efficiency, and performance with a unique fin design arrangement. The current analysis also observed a considerable enhancement in fin performance and efficiency. This shows that the novel fin design proposed here can be an innovative step in the fin design, which enhances the heat transfer rate for low-temperature range applications. Also, it reduces manufacturing costs and provides a simple design solution with improved robustness without compromising fin performance.

Discussion on reasons of getting higher amplitudes on responses for low Fourier numbers for both geometries under wet conditions

Thermal relaxation time in heat wave propagation has a broader scope in any transient heat transfer analysis. The nature of the heat wave propagation and its amplitude depends on the fin's thermal relaxation time and initial temperature, along with other fin parameters and dimensionless numbers. At different base boundary conditions and due to the non-Fourier heat conduction, a noticeably higher amplitude on responses for low Fourier value was seen during the transient heat transfer response in the wet fin due to the following reasons:

1. The difference in the temperature response between Fourier and non-Fourier models is remarkable at lower values of Fourier number, τ due to dominating a finite speed of heat wave propagation for the non-Fourier model. This difference gradually diminishes with higher values of τ and the speed of the thermal wave in non-Fourier model approaches that of the Fourier one.
2. Considering the non-Fourier analysis, with lower values of the Biot number, the wet fin surface exhibits more transient effects with higher amplitude and waviness. The smoothness of the curve may be due to the convective heat transfer occurring at the base boundary surface.
3. In a unique fin design study, results show that, as the Fourier number, τ , increases, the spatial temperature in the fin approaches a stable temperature to reach a steady temperature. However, at lower values of Fourier number, the curve exhibits a peculiar nature for dominating non-Fourier nature towards the middle part of the curve, indicating a slower heat conduction rate.
4. At a lower value of Fourier number τ , the non-Fourier temperature response looks sinusoidal for the hyperbolic governing equation. The dehumidification effect in wet

fin surfaces enhances the waviness and increases the amplitudes in the thermal wave when compared with dry fin surfaces. It can be concluded here that a wet fin surface is more sensitive to non-Fourier heat conduction than a dry surface.

5. It can be noticed that the convective fin base condition gives a smoother temperature response than the isothermal fin base condition because of the less restricted movement of the heat wave.
6. The non-Fourier heat transfer dominates with the condensation due to the more heat transfer at the fin surface for the evolving latent heat of moisture condensation.
7. The difference in temperature between the fin surface and fin base in non-Fourier heat transfer is significantly less during the initial period.

CHAPTER-5

Conclusion

The transient temperature response in the longitudinal and spine fin of constant thickness with dehumidification effect for conducting heat according to Fourier and non-Fourier laws is determined analytically. Realistic boundary conditions like isothermal and convective bases with convective fin tip conditions utilize to analyze the fin's Fourier and non-Fourier temperature responses. A closed-form solution develops to compute the temperature distribution, the overall fin efficiency, and fin effectiveness considering two fin geometries under a wet condition.

From the main objectives of this study and after careful observation of various significant results from Chapters 3 and 4, the following conclusions can be drawn:

1. The present analysis can also determine the transient response for the heat transfers involving the classical Fourier's law of heat conduction.
2. Notably, the condensation effect on the fin surface enhances waviness in transient temperature response in non-Fourier heat conduction. The amplitude of the temperature distribution curve depends upon the Vernotte number, fin surface condition, and boundary condition at the base.
3. The fin efficiency with the non-Fourier heat transfer becomes maximum when the temperature between the fin base and tip is minimum. The fin efficiency is always more in dry surface conditions.

4. The new fin design arrangement yields better thermal performance and fin efficiency than the other fin geometries, and it has a prominent effect on the temperature response curve.
5. The overall fin efficiency of the longitudinal fin is higher than that of the pin fin under both dry and wet surface conditions.
6. It is worth noting that, for an accurate analysis of wet fin surface transient heat conduction, a non-Fourier approach is always essential as it is a generalized form.
7. The present analysis of non-Fourier heat transfers determining the performance parameters of wet fins is helpful for the correct fin design information under transient behavior conditions.

Future Scope

Any research work is a perpetual task; researchers always explore futuristic opportunities for the betterment of humankind. The analytical study concludes a certain academic point in the present study. However, fin heat transfer considering transient heat conduction can be a milestone in the futuristic journey in upcoming heat transfer applications. In the emerging application, the composite mini-micro size fin designs with a minimal thermal relaxation time might be essential in the near future task.

Apart from this, a few things are expected to be considered in the future study scope: The combination of different fin geometries, fin surface finish, and it's fitting while using them in arrays. It will be worth carrying out experimentation for the confirmation of the results obtained from the analytical study. A sophisticated experimental setup is required as the transient effect can be observed for a very small duration.

References

- [1] B. Kundu, A new methodology for determination of an optimum fin shape under dehumidifying conditions, *Int. J. Refrig.* 33 (2010) 1105–1117. <https://doi.org/10.1016/j.ijrefrig.2010.04.001>.
- [2] Y.J. Chang, C.C. Wang, A generalized heat transfer correlation for louver fin geometry, *Int. J. Heat Mass Transf.* 40 (1997) 533–544. [https://doi.org/10.1016/0017-9310\(96\)00116-0](https://doi.org/10.1016/0017-9310(96)00116-0).
- [3] A.R.A. Khaled, M. Siddique, N.I. Abdulhafiz, A.Y. Boukhary, Recent advances in heat transfer enhancements: A review report, *Int. J. Chem. Eng.* 2010 (2010). <https://doi.org/10.1155/2010/106461>.
- [4] E. Yu, Y. Joshi, Heat transfer enhancement from enclosed discrete components using pin-fin heat sinks, *Int. J. Heat Mass Transf.* 45 (2002) 4957–4966. [https://doi.org/10.1016/S0017-9310\(02\)00200-4](https://doi.org/10.1016/S0017-9310(02)00200-4).
- [5] C.N. Lin, J.Y. Jang, A two-dimensional fin efficiency analysis of combined heat and mass transfer in elliptic fins, *Int. J. Heat Mass Transf.* 45 (2002) 3839–3847. [https://doi.org/10.1016/S0017-9310\(02\)00086-8](https://doi.org/10.1016/S0017-9310(02)00086-8).
- [6] A. Sasmal, S.C. Mishra, Analysis of non-Fourier conduction and radiation in a differentially heated 2-D square cavity, *Int. J. Heat Mass Transf.* 79 (2014) 116–125. <https://doi.org/10.1016/j.ijheatmasstransfer.2014.08.010>.
- [7] B. Kundu, Approximate analytical method for prediction of performance and optimum dimensions of pin fins subject to condensation of quiescent vapor, *Int. J. Refrig.* 32 (2009) 1657–1671. <https://doi.org/10.1016/j.ijrefrig.2009.04.006>.
- [8] C. Cattaneo, A form of heat conduction equation which eliminates the paradox of instantaneous propagation, *Comput. Rendus.* 247 (1958) 431–433.
- [9] M.N. Özışık, D.Y. Tzou, On the wave theory in heat conduction, *J. Heat Transfer.* 116 (1994) 526–535. <https://doi.org/10.1115/1.2910903>.
- [10] N. V. Suryanarayana, Transient Response of Straight Fins., *Am. Soc. Mech. Eng.* (1975) 417–423.

- [11] W.-N.J. Chang Joo Cho, Non-Fourier heat conduction in a slab subjected to periodic surface heating. *J. Korean Phy soc.* 2000;36:209-14., *J. Korean Phy Soc.* 36 (2000) 209–14.
- [12] F. De Monte, Transient heat conduction in one-dimensional composite slab. A “natural” analytic approach, *Int. J. Heat Mass Transf.* 43 (2000) 3607–3619. [https://doi.org/10.1016/S0017-9310\(00\)00008-9](https://doi.org/10.1016/S0017-9310(00)00008-9).
- [13] B. Kundu, K.S. Lee, A non-Fourier analysis for transmitting heat in fins with internal heat generation, *Int. J. Heat Mass Transf.* 64 (2013) 1153–1162. <https://doi.org/10.1016/j.ijheatmasstransfer.2013.05.057>.
- [14] H. Ahmadikia, M. Rismanian, Analytical solution of non-Fourier heat conduction problem on a fin under periodic boundary conditions, *J. Mech. Sci. Technol.* 25 (2011) 2919–2926. <https://doi.org/10.1007/s12206-011-0720-5>.
- [15] C.H. Huang, Y.L. Tsai, A transient 3-D inverse problem in imaging the time-dependent local heat transfer coefficients for plate fin, *Appl. Therm. Eng.* 25 (2005) 2478–2495. <https://doi.org/10.1016/j.applthermaleng.2004.12.003>.
- [16] B. Kundu, D. Barman, S. Debnath, An analytical approach for predicting fin performance of triangular fins subject to simultaneous heat and mass transfer, *Int. J. Refrig.* 31 (2008) 1113–1120. <https://doi.org/10.1016/j.ijrefrig.2008.01.007>.
- [17] J.L. Threlkeld, *Thermal Environmental Engineering*, 2nd ed, Prentice-Hall, 1970.
- [18] M. Turkyilmazoglu, Efficiency of heat and mass transfer in fully wet porous fins: Exponential fins versus straight fins, *Int. J. Refrig.* 46 (2014) 158–164. <https://doi.org/10.1016/j.ijrefrig.2014.04.011>.
- [19] M. Hatami, D.D. Ganji, Investigation of refrigeration efficiency for fully wet circular porous fins with variable sections by combined heat and mass transfer analysis, *Int. J. Refrig.* 40 (2014) 140–151. <https://doi.org/10.1016/j.ijrefrig.2013.11.002>.
- [20] M. F.C., *Fin Efficiency with combined heat and mass transfer*, ASHRAE. Trans 81:3 (n.d.).
- [21] M.H. Sharqawy, S.M. Zubair, Efficiency and optimization of a straight rectangular fin with combined heat and mass transfer, *Heat Transf. Eng.* 29 (2008) 1018–1026.

- <https://doi.org/10.1080/01457630802243030>.
- [22] B. Kundu, An analytical study of the effect of dehumidification of air on the performance and optimization of straight tapered fins, *Int. Commun. Heat Mass Transf.* 29 (2002) 269–278. [https://doi.org/10.1016/S0735-1933\(02\)00317-2](https://doi.org/10.1016/S0735-1933(02)00317-2).
- [23] C.H. Huang, Y.L. Chung, The determination of optimum shapes for fully wet annular fins for maximum efficiency, *Appl. Therm. Eng.* 73 (2014) 438–448. <https://doi.org/10.1016/j.applthermaleng.2014.07.071>.
- [24] M.H. Kim, H. Kim, D.R. Kim, K.S. Lee, A novel louvered fin design to enhance thermal and drainage performances during periodic frosting/defrosting conditions, *Energy Convers. Manag.* 110 (2016) 494–500. <https://doi.org/10.1016/j.enconman.2015.11.028>.
- [25] C.B. Sobhan, S.P. Venkateshan, K.N. Seetharamu, Experimental analysis of unsteady free convection heat transfer from horizontal fin arrays Eine experimentelle Untersuchung der Wärmeübertragung bei instationärer freier Konvektion an horizontalen Rippenanordnungen, *Wärme- Und Stoffübertragung.* 24 (1989) 155–160.
- [26] R.J. Su, J.J. Hwang, Transient analysis of two-dimensional cylindrical pin fin with tip convective effects, *Heat Transf. Eng.* 20 (1999) 57–63. <https://doi.org/10.1080/014576399271420>.
- [27] S.Z. Mostafa H. Sharqawy, Efficiency and optimization of a straight rectangular fin with combined heat and mass transfer., . . *Heat Transf. Eng.* 29 (2011) 1018–26.
- [28] C. Li, J. Li, H. Zhang, Airside fin efficiencies for finned-tube heat exchangers with forced convection, *Sci. China Technol. Sci.* 54 (2011) 2468–2474. <https://doi.org/10.1007/s11431-011-4412-2>.
- [29] J.S. Loh, I.A. Azid, K.N. Seetharamu, G.A. Quadir, Fast transient thermal analysis of Fourier and non-Fourier heat conduction, *Int. J. Heat Mass Transf.* 50 (2007) 4400–4408. <https://doi.org/10.1016/j.ijheatmasstransfer.2007.03.021>.
- [30] L.W. Zhang, S. Balachandar, D.K. Tafti, F.M. Najjar, Heat transfer enhancement mechanisms in inline and staggered parallel-plate fin heat exchangers, *Int. J. Heat Mass Transf.* 40 (1997) 2307–2325. [https://doi.org/10.1016/S0017-9310\(96\)00303-1](https://doi.org/10.1016/S0017-9310(96)00303-1).

- [31] R. Das, S.C. Mishra, T.B.P. Kumar, R. Uppaluri, An inverse analysis for parameter estimation applied to a non-fourier conduction-radiation problem, *Heat Transf. Eng.* 32 (2011) 455–466. <https://doi.org/10.1080/01457632.2010.506167>.
- [32] S. Kiwan, M.A. Al-Nimr, Using porous fins for heat transfer enhancement, *J. Heat Transfer.* 123 (2001) 790–795. <https://doi.org/10.1115/1.1371922>.
- [33] M.H. Sharqawy, S.M. Zubair, Efficiency and optimization of an annular fin with combined heat and mass transfer - An analytical solution, *Int. J. Refrig.* 30 (2007) 751–757. <https://doi.org/10.1016/j.ijrefrig.2006.12.008>.
- [34] J.-Y.J. Chien-Nan Lin, A two dimensional fin efficiency analysis of combined heat and mass transfer in elliptic fins., *Int. J. Heat Mass Transf.* 45: (2002) 3839–47.
- [35] S. Mosayebidorcheh, M. Farzinpoor, D.D. Ganji, Transient thermal analysis of longitudinal fins with internal heat generation considering temperature-dependent properties and different fin profiles, *Energy Convers. Manag.* 86 (2014) 365–370. <https://doi.org/10.1016/j.enconman.2014.05.033>.
- [36] D.P. Vishwakarma V, Das AK, Analysis of non-Fourier heat conduction using smoothed particle hydrodynamics., *Appl Therm Eng.* 31 (2011) 2963–70.
- [37] S.M.Z. Mostafa H., Sharqawy, Abdurrahman Moinuddin, Heat and mass transfer from annular fins of different cross-sectional area. Part I. temperature distribution and fin efficiency., *Int. J. Refrig.* 35 (2012) 365–76.
- [38] Cho and Juhng, No Title, (n.d.).
- [39] B. Kundu, K.S. Lee, A novel analysis for calculating the smallest envelope shape of wet fins with a nonlinear mode of surface transport, *Energy.* 44 (2012) 527–543. <https://doi.org/10.1016/j.energy.2012.05.049>.
- [40] S.M.Z. Abdurrahman M, Mostafa H, Sharqawy, Heat and mass transfer from annular fins of different cross-sectional area. Part II. Optimal dimensions of fins., *Int. J. Refrig.* 35 (2012) 377–85.
- [41] W. Pirompugd, C.C. Wang, S. Wongwises, Finite circular fin method for heat and mass transfer characteristics for plain fin-and-tube heat exchangers under fully and partially wet surface conditions, *Int. J. Heat Mass Transf.* 50 (2007) 552–565.

- <https://doi.org/10.1016/j.ijheatmasstransfer.2006.07.017>.
- [42] E.A.M. Elshafei, Natural convection heat transfer from a heat sink with hollow/perforated circular pin fins, *Energy*. 35 (2010) 2870–2877.
<https://doi.org/10.1016/j.energy.2010.03.016>.
- [43] S.A. Hazarika, D. Bhanja, S. Nath, B. Kundu, Analytical solution to predict performance and optimum design parameters of a constructal T-shaped fin with simultaneous heat and mass transfer, *Energy*. 84 (2015) 303–316.
<https://doi.org/10.1016/j.energy.2015.02.102>.
- [44] A.A. Sertkaya, Ş. Bilir, S. Kargici, Experimental investigation of the effects of orientation angle on heat transfer performance of pin-finned surfaces in natural convection, *Energy*. 36 (2011) 1513–1517.
<https://doi.org/10.1016/j.energy.2011.01.014>.
- [45] Kundu, B., Biswas, P., & Lee, K. S. (2017). Establishment of modified-one-dimensional and two-dimensional models for two-directional heat conduction in a wet fin assembly. *Heat Transfer Engineering*, 38(2), 190-205.
- [46] S. Singh, D. Kumar, K.N. Rai, Analytical solution of Fourier and non-Fourier heat transfer in longitudinal fin with internal heat generation and periodic boundary condition, *Int. J. Therm. Sci.* 125 (2018) 166–175.
<https://doi.org/10.1016/j.ijthermalsci.2017.11.029>.
- [47] B. Kundu, A. Miyara, An analytical method for determination of the performance of a fin assembly under dehumidifying conditions: A comparative study, *Int. J. Refrig.* 32 (2009) 369–380. <https://doi.org/10.1016/j.ijrefrig.2008.03.011>.
- [48] I. Rahbari, F. Mortazavi, M.H. Rahimian, High order numerical simulation of non-Fourier heat conduction: An application of numerical Laplace transform inversion, *Int. Commun. Heat Mass Transf.* 51 (2014) 51–58.
<https://doi.org/10.1016/j.icheatmasstransfer.2013.12.003>.
- [49] Y. Xia, A.M. Jacobi, An exact solution to steady heat conduction in a two-dimensional slab on a one-dimensional fin: Application to frosted heat exchangers, *Int. J. Heat Mass Transf.* 47 (2004) 3317–3326. <https://doi.org/10.1016/j.ijheatmasstransfer.2004.01.019>.

- [50] B.M. Sabbaghi S, Rezaii A, Shahri Gh. R, Mathematical analysis for Transfer., the efficiency of a semi-spherical fin with simultaneous heat and mass, , *Int. J. Refrig.* 34 (2011) 1877–82.
- [51] M. Hatami, G.R. Mehdizadeh Ahangar, D.D. Ganji, K. Boubaker, Refrigeration efficiency analysis for fully wet semi-spherical porous fins, *Energy Convers. Manag.* 84 (2014) 533–540. <https://doi.org/10.1016/j.enconman.2014.05.007>.
- [52] S. Saedodin, M. Torabi, Algebraically Explicit Analytical Solution of Three-Dimensional Hyperbolic Heat Conduction Equation, *Adv. Theor. Appl. Mech.* 3 (2010) 369–383.
- [53] S.C. Mishra, H. Sahai, Analyses of non-Fourier heat conduction in 1-D cylindrical and spherical geometry - An application of the lattice Boltzmann method, *Int. J. Heat Mass Transf.* 55 (2012) 7015–7023. <https://doi.org/10.1016/j.ijheatmasstransfer.2012.07.014>.
- [54] B. Kundu, K.S. Lee, Fourier and non-Fourier heat conduction analysis in the absorber plates of a flat-plate solar collector, *Sol. Energy.* 86 (2012) 3030–3039. <https://doi.org/10.1016/j.solener.2012.07.011>.
- [55] L. Zhang, X. Shang, Analytical solution to non-Fourier heat conduction as a laser beam irradiating on local surface of a semi-infinite medium, *Int. J. Heat Mass Transf.* 85 (2015) 772–780. <https://doi.org/10.1016/j.ijheatmasstransfer.2015.02.024>.
- [56] D.R. Harper, W.B. Brown, *Mathematical Equations for Heat Conduction in the Fins of Air Cooled Engines*, (1922) No. 158.
- [57] A. Acosta-Iborra, A. Campo, Approximate analytic temperature distribution and efficiency for annular fins of uniform thickness, *Int. J. Therm. Sci.* 48 (2009) 773–780. <https://doi.org/10.1016/j.ijthermalsci.2008.05.012>.
- [58] W. Wen-Jyi, C. Cha'o-Kuang, Transient response of a spiral fin with its base subjected to a sinusoidal form in temperature, *Comput. Struct.* 34 (1990) 161–169. [https://doi.org/10.1016/0045-7949\(90\)90310-X](https://doi.org/10.1016/0045-7949(90)90310-X).
- [59] Gardner, K. A. (1945). Efficiency of extended surface. *Transactions of the American Society of Mechanical Engineers*, 67(8), 621–628.
- [60] J.W. Yu Chen, Haoran Chen, Hao Zeng, Jianjun Zhu, Kai Chen , Zhenyu Cui, *Structural*

- optimization design of sinusoidal wavy plate fin heat sink with crosscut by Bayesian optimization, *Appl. Therm. Eng.* 213 (2022) 118755.
- [61] P.A. Wankhade, B. Kundu, R. Das, Establishment of non-Fourier heat conduction model for an accurate transient thermal response in wet fins, *Int. J. Heat Mass Transf.* 126 (2018) 911–923. <https://doi.org/10.1016/j.ijheatmasstransfer.2018.05.094>.
- [62] O.T. Heggs PJ, Design charts for radial rectangular fins in terms of performance ratio and maximum effectiveness., *Appl. Therm. Eng.* 24(8e9 (2004) 1341.
- [63] R. Das, B. Kundu, Direct and inverse approaches for analysis and optimization of fins under sensible and latent heat load, *Int. J. Heat Mass Transf.* 124 (2018) 331–343. <https://doi.org/10.1016/j.ijheatmasstransfer.2018.03.059>.
- [64] P. Naphon, S. Klangchart, S. Wongwises, Numerical investigation on the heat transfer and flow in the mini-fin heat sink for CPU, *Int. Commun. Heat Mass Transf.* 36 (2009) 834–840. <https://doi.org/10.1016/j.icheatmasstransfer.2009.06.010>.
- [65] S.R. Hosseini, M. Sheikholeslami, M. Ghasemian, D.D. Ganji, Nanofluid heat transfer analysis in a microchannel heat sink (MCHS) under the effect of magnetic field by means of KKL model, *Powder Technol.* 324 (2018) 36–47. <https://doi.org/10.1016/j.powtec.2017.10.043>.
- [66] W. Roetzel, N. Putra, S.K. Das, Experiment and analysis for non-Fourier conduction in materials with non-homogeneous inner structure, *Int. J. Therm. Sci.* 42 (2003) 541–552. [https://doi.org/10.1016/S1290-0729\(03\)00020-6](https://doi.org/10.1016/S1290-0729(03)00020-6).
- [67] B. Abdel-Hamid, Modelling non-Fourier heat conduction with periodic thermal oscillation using the finite integral transform, *Appl. Math. Model.* 23 (1999) 899–914. [https://doi.org/10.1016/S0307-904X\(99\)00017-7](https://doi.org/10.1016/S0307-904X(99)00017-7).
- [68] B. Kundu, R. Das, P.A. Wankhade, K.S. Lee, Heat transfer improvement of a wet fin under transient response with a unique design arrangement aspect, *Int. J. Heat Mass Transf.* 127 (2018) 1239–1251. <https://doi.org/10.1016/j.ijheatmasstransfer.2018.08.110>.
- [69] M. Sheikholeslami, D.D. Ganji, Influence of electric field on Fe₃O₄- water nanofluid radiative and convective heat transfer in a permeable enclosure, *J. Mol. Liq.* 250 (2018)

- 404–412. <https://doi.org/10.1016/j.molliq.2017.12.028>.
- [70] M. Turkyilmazoglu, Heat transfer from warm water to a moving foot in a footbath, *Appl. Therm. Eng.* 98 (2016) 280–287. <https://doi.org/10.1016/j.applthermaleng.2015.12.027>.
- [71] Q.M. Fan, W.Q. Lu, A new numerical method to simulate the non-Fourier heat conduction in a single-phase medium, *Int. J. Heat Mass Transf.* 45 (2002) 2815–2821. [https://doi.org/10.1016/S0017-9310\(01\)00364-7](https://doi.org/10.1016/S0017-9310(01)00364-7).
- [72] Singh, S., Kumar, D., & Rai, K. N. (2018). Analytical solution of Fourier and non-Fourier heat transfer in longitudinal fin with internal heat generation and periodic boundary condition. *International Journal of Thermal Sciences*, 125, 166-175.
- [73] Oguntala, G., Sobamowo, G., & Abd-Alhameed, R. (2019). Numerical analysis of transient response of convective-radiative cooling fin with convective tip under magnetic field for reliable thermal management of electronic systems. *Thermal Science and Engineering Progress*, 9, 289-298.
- [74] Ndlovu, P. L., & Moitsheki, R. J. (2019). Analysis of temperature distribution in radial moving fins with temperature dependent thermal conductivity and heat transfer coefficient. *International Journal of Thermal Sciences*, 145, 106015.
- [75] Oguntala, G., Abd-Alhameed, R., & Ngala, M. (2019). Transient thermal analysis and optimization of convective-radiative porous fin under the influence of magnetic field for efficient microprocessor cooling. *International Journal of Thermal Sciences*, 145, 106019.
- [76] Kheirandish, Z., Kharati-Koopae, M., & Omidvar, A. (2020). Numerical study into the fin performance subjected to different periodic base temperatures employing Fourier and non-Fourier heat conduction models. *International Communications in Heat and Mass Transfer*, 114, 104562.
- [77] Liu, Y., Li, L., & Zhang, Y. (2020). Numerical simulation of non-Fourier heat conduction in fins by lattice Boltzmann method. *Applied Thermal Engineering*, 166, 114670.

- [78] Das, R., & Kundu, B. (2021). Simultaneous estimation of heat generation and magnetic field in a radial porous fin from surface temperature information. *International Communications in Heat and Mass Transfer*, 127, 105497.
- [79] Kundu, B., & Yook, S. J. (2021). An accurate approach for thermal analysis of porous longitudinal, spine and radial fins with all nonlinearity effects - analytical and unified assessment. *Applied Mathematics and Computation*, 402, 126124.
- [80] Keerthi, M. L., Gireesha, B. J., & Sowmya, G. (2022). Numerical investigation of efficiency of fully wet porous convective-radiative moving radial fin in the presence of shape-dependent hybrid nanofluid. *International Communications in Heat and Mass Transfer*, 138, 106341.
- [81] Tan, Z., Duan, K., Xiu, W., Liu, X., Wang, Y., Wang, Q., & Chu, W. (2022). Enhancement mechanism on heat and mass transfer of tall fin with cycloid thermosyphon loop. *International Journal of Heat and Mass Transfer*, 198, 123432.
- [82] Kundu, B., & Yook, S. J. (2023). Analytical model for extremum analysis of moistened fins involving all nonlinear energy exchange processes. *Case Studies in Thermal Engineering*, 41, 102691.
- [83] Goud, J. S., Srilatha, P., Kumar, R. V., Sowmya, G., Gamaoun, F., Nagaraja, K. V., & Eldin, S. M. (2023). Heat transfer analysis in a longitudinal porous trapezoidal fin by non-Fourier heat conduction model: An application of artificial neural network with Levenberg - Marquardt approach. *Case Studies in Thermal Engineering*, 49, 103265.
- [84] Gamaoun, F., Abdulrahman, A., Sowmya, G., Kumar, R., Khan, U., Alotaibi, A. M., Kumar R. V. (2023). Non-Fourier heat transfer in a moving longitudinal radiative-convective dovetail fin. *Case Studies in Thermal Engineering*, 41, 102623.


10/03/2023